STRUCTURAL ANALYSIS OF FRACTURES AROUND UNDERGROUND EXCAVATIONS ON A WITWATERSRAND GOLD-MINE

by

Rüdiger Welf Olgert Kersten

Submitted in partial fulfilment of
the requirements for the degree
of Master of Science

in the

Faculty of Science

University of Pretoria

December 1969

ABSTRACT

The interpretation of faults and joints on the basis of stresses in the earth's crust has been attempted on many occasions. The main problem encountered in such interpretations has been that the physical conditions, and the stress field, during the period of origin of these faults were imperfectly known.

New information has become available with regard to the mechanisms involved in fracture processes, primarily in the development of the modified Griffith criterion of fracture initiation.

The validity of this criterion is tested by comparing orientations of fractures as predicted with those measured in a known environment.

Fractures in the hanging wall of a stope were measured on a gold-mine in the Klerksdorp area.

Comparison of predicted and measured orientations shows that the limits within which the orientation of fractures must be, can be predicted. However, minor variations within these limits indicate that a more elaborate model than an idealised slit in an elastic medium is necessary.

The modified Griffith's criterion of fracture is used to analyse the history of faulting at the Loraine Gold Mine in the Orange Free State. The studies show that it is possible to place certain limiting conditions on the physical properties of the material, and the stress fields existing at the time of origin of the fault systems.

SAMEVATTING

Die verklaring van die ontstaan van verskuiwings en nate op grond van 'n analise van die spanningsverspreiding in die aardkors lewer probleme op in die opsig dat die eienskappe van die gesteentes gedurende die proses van verskuiwing nie in besonderhede bekend is nie.

Nuwe inligting met betrekking tot die ontstaan van krake, veral die gewysigde Griffith-kriterium kan heelwat lig op die saak werp.

Die betroubaarheid van die Griffith-kriterium word hier getoets deur voorspellings met metings in 'n bekende spanningsveld te vergelyk.

Die orientasie van krake in die dak van 'n afbouplek in 'n goudmyn in die Klerksdorpgebied word vergelyk met die wat voorspel word deur gebruik te maak van die Griffith-kriterium.

Die vergelyking toon dat die grense van orientasie waarin die gemete krake moet voorkom, voorspel kan word. Klein afwykings binne die grense toon egter dat 'n meer uitgebreide model gebruik moet word instede van die van 'n geidealiseerde gleuf in 'n elastiese medium.

Die verskuiwings soos gevind in Loraine-goudmyn in die Vrystaat is herondersoek. Met behulp van die Griffith-kriterium is dit moontlik om sekere grense te plaas op die spanningveld en die fisiese toestande van die gesteentes tydens die ontstaan van die verskuiwings.

STRUCTURAL ANALYSIS OF FRACTURES AROUND UNDERGROUND EXCAVATIONS ON A WITWATERSRAND GOLD-MINE

C O N T E N T S

/6. Prediction .....

****

1. INTRODUCTION.

Anderson (1951) used the Navier-Coulomb fracture criterion to explain the dynamics of faulting and dyke formation. From this he could reconstruct the changes in the stress systems which gave rise to the faults and dykes present in Great Britain.

Since 1951 a vast amount of additional knowledge has been gained with regard to the mechanics of fracturing processes. In this paper it will be attempted to use this knowledge in a similar way as Anderson has done and to find out whether it can be applied successfully in structural analysis.

Jaeger (1964, pp. 75-95) gives a summary of failure criteria at present in use for predicting the strength of materials, or, alternatively, the reconstruction of the stress field from an existing fracture pattern by means of structural analysis.

Fracturing criteria can be subdivided into two categories, viz:

(a) Stress failure criteria which are based on :-

(i) the maximum shear-stress theory (Navier-Coulomb).

(ii) Mohr's theory of fracture.

(iii) The Griffith theory, and

(iv) yield criteria.

(b) Strain failure criteria in connection with which the maximum shear-strain theory is the most used.

Of the criteria mentioned above, Mohr's theory of fracture, the yield criteria, and the maximum shear-stress theory have not improved over the last twenty years. It is mainly the Griffith fracture criterion for

brittle materials which has been developed extensively.

The purpose of this paper is to use the Griffith fracture criterion, which attempts to explain the mechanism of fracture formation, in structural analysis.

An attempt in this direction was made by Roering (1967) and the conclusion of his investigation was that "en echelon" crack arrays are a first order phenomenon, and not of a second order as hitherto assumed. The correctness of his conclusion is not relevant; the main point is the importance of using the newly gained knowledge in structural analysis.

However, before using this criterion, its validity has to be established. Hoek (1965) has proved that it could be used for predicting the strength of prepared specimens.

During 1964 the Chamber of Mines of South Africa initiated a research programme into the nature and behaviour of fractured rock around underground excavations on the Witwatersrand gold-mines.

In the course of this investigation numerous fractures were measured which could be used to test the Griffith criterion on a larger scale where it was still possible to calculate the stress distribution necessary for the application of this criterion.

Firstly, the locality at which the measurements were taken is described. This is followed by a detailed description of the fractures.

The next step is to discuss the fracture criteria listed above and the calculation of the stress distribution is mentioned briefly.

A comparison between the measured and the predicted orientation and the nature of fractures follows and some conclusions are drawn. The main purpose of this thesis is to use the Griffith fracture criterion in structural analysis; a certain geological area is re-investigated with the conclusions mentioned above in mind.

2. METHODS OF STUDY AND SOURCES OF INFORMATION:

The initial step was to determine whether the fractures around underground excavations showed any systematic behaviour. After visits to a number of mines in the Witwatersrand System it was found that this is indeed the case. The next step was to select a site which was favourably situated.

A favourable situation means that :-

(a) The geometry must be such that it is possible to calculate the stress distribution to a certain degree of accuracy. This implies that adjacent mining excavations should be far enough removed so as to exclude any possible interference between the two induced stress fields.

(b) The rock mass must behave essentially in an elastic manner.

(c) No relict tectonic forces should be active in this area. Measurement of the deformed rocks in bore-holes can be used to determine the virgin rock stress, (Bonnechere and Fairhurst, 1968, p.520) or fractures in the vicinity of the excavation should follow their geometry closely; if this is not the case, relict tectonic forces, or superimposed stresses from adjacent excavations, are active.

A site satisfying the above requirements was found at Hartebeestfontein Gold-mine in the Western Transvaal (Fig. 1).

Comparison between measured and predicted deformations caused by mining showed that the rock mass behaved in an essentially elastic manner in the area (unpublished report by Kersten). Stope 29 S 11 (Fig. 2) was far enough removed from other mined-out areas in order to prevent possible interaction between induced stress fields and a study of fractures in the area showed no sign of still active relict tectonic stresses.

Plates I to III show the appearance of the fractures in the hanging wall of the stope. Their orientation and their spacing were measured and their surface features were described as the stope face advanced as shown in Fig. 3.

This stope geometry was then used to calculate the stress distribution, on the assumption that the material behaves in an elastic manner.

The calculated stress distribution was then used, in conjunction with the modified Griffith fracture criterion, to predict the orientation and the extent of the fracture zone in the immediate vicinity of the stope face.

3. THE KLERKSDORP GOLD-FIELD:

3.1. Definition and location of area.

The Klerksdorp area is about 100 miles south-west of Johannesburg and 70 miles north-west of the Orange Free State gold-fields (Fig. 1).

The Hartebeestfontein Gold-mine (Fig. 2) is one of five major gold producers in this area.

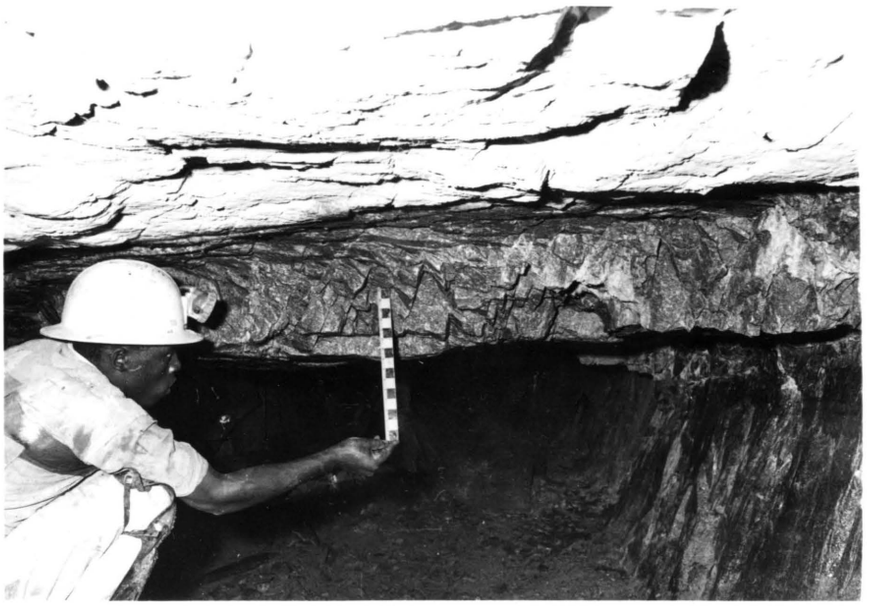

PLATE I: Fractures in the hanging wall of Stope 29 S 11 N1.

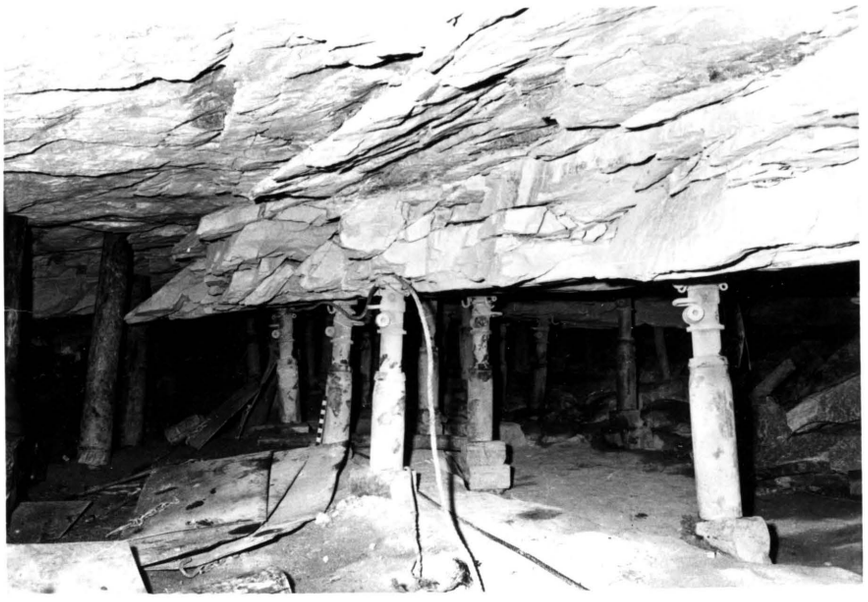

PLATE II: Fractures in the hanging wall of Stope 29 S 11 N2

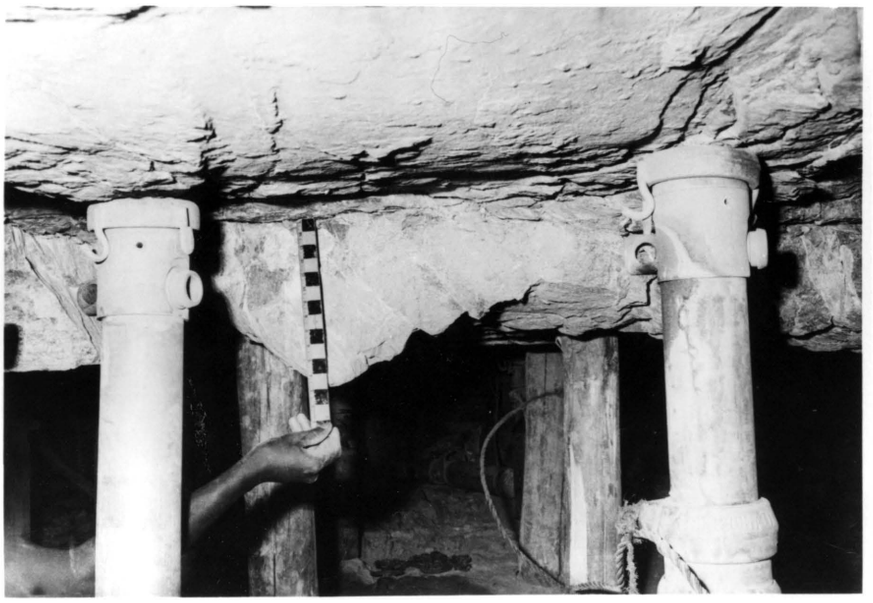

PLATE III: Fractures in the hanging wall of Stope 29 S 11 N1

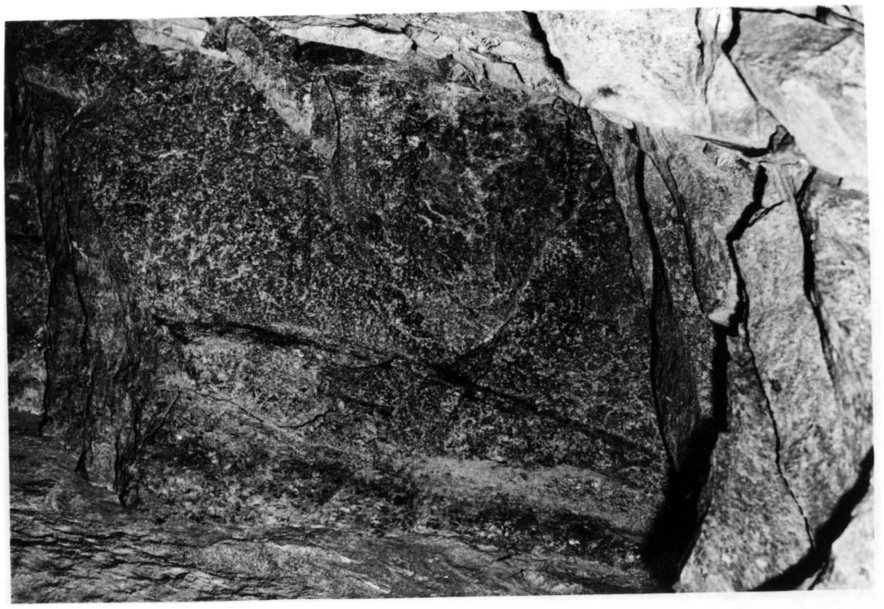

PLATE IV: Typical surface of a Class I fracture

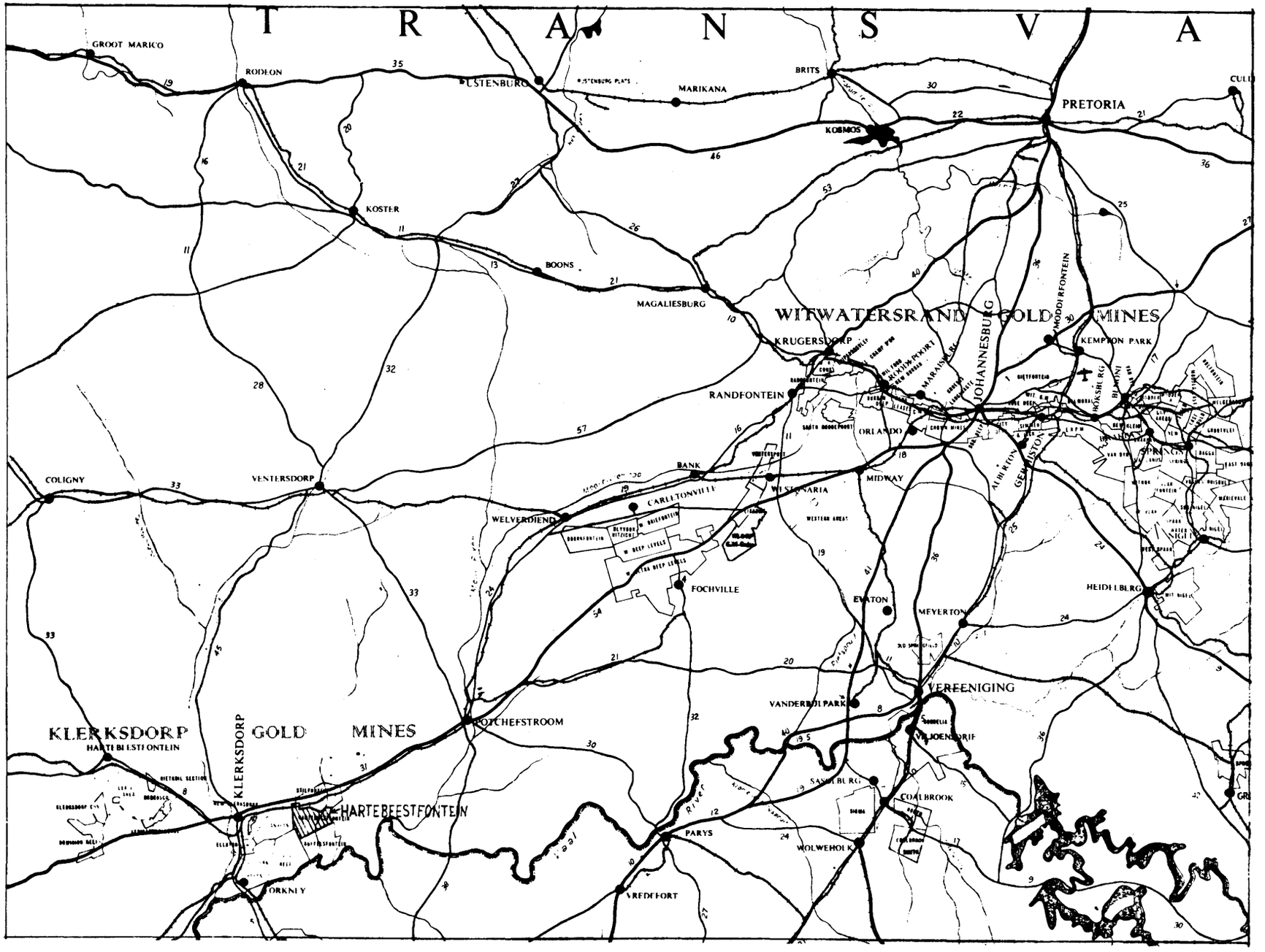

FIGURE 1.

PLAN SHOWING THE LOCATION OF HARTEBEESTFONTEIN GOLD MINING CO. LTD. IN THE TRANSVAAL

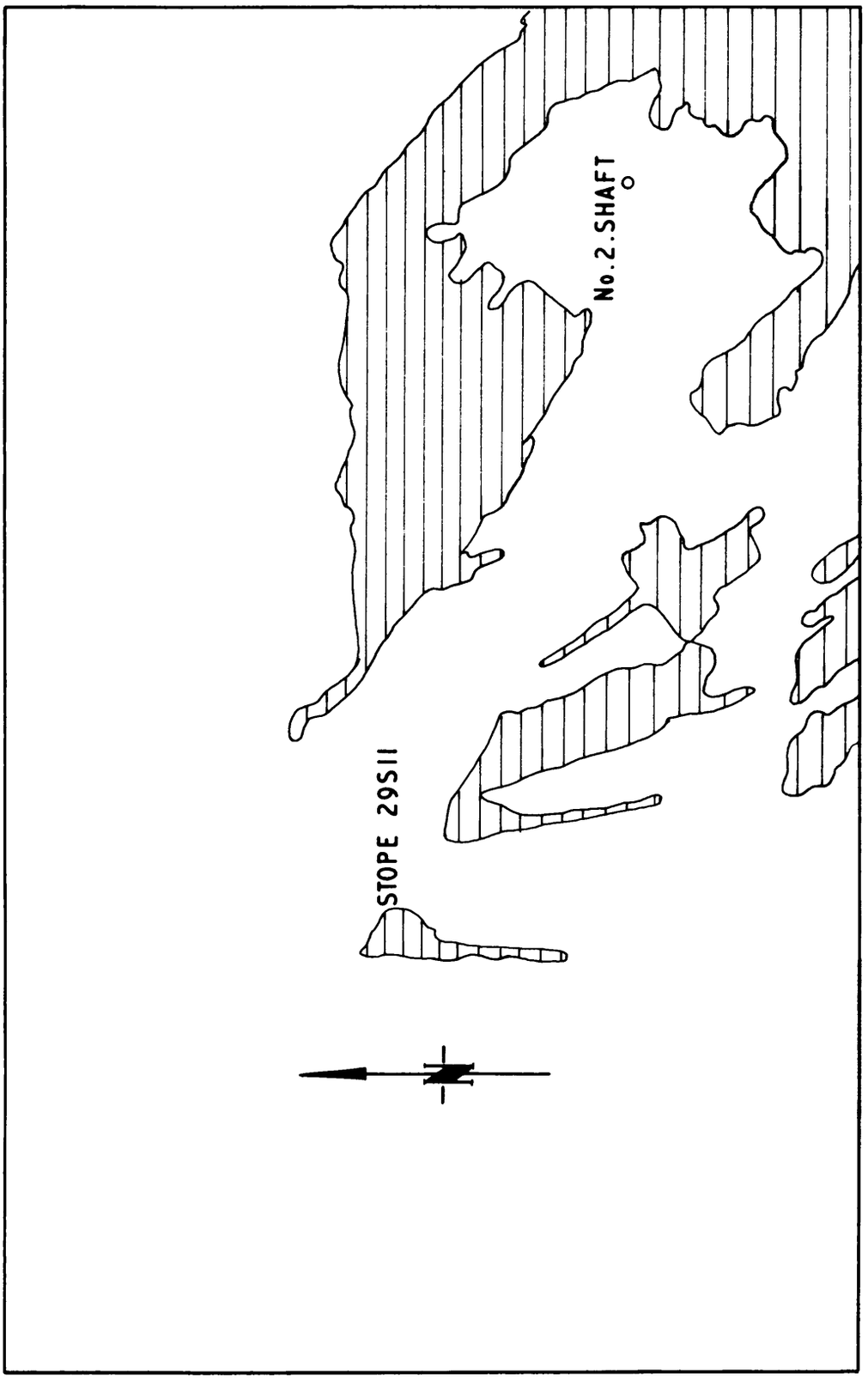

FIGURE 2

UNDERGROUND WORKINGS AS AT 30/6/65 AT HARTEBEESTFONTEIN GOLD MINING CO.LTD. AND LOCATION OF STOPE 29S11.

SCALE 1:10,000.

RM.10.

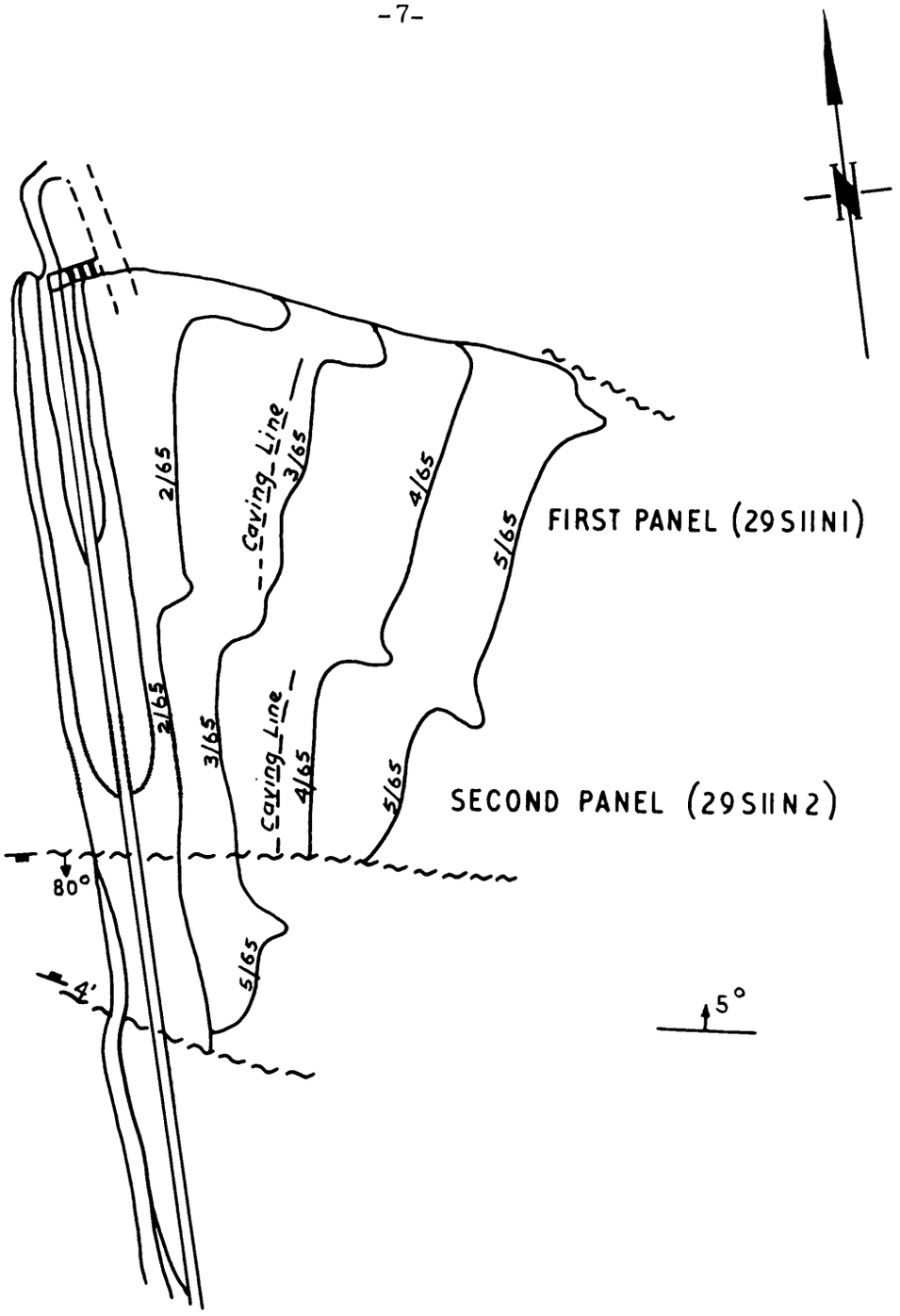

FIGURE 3

OUTLINE OF STOPE 29S11 FOR THE PERIOD FROM 20-2-65 TO 20-5-65.

SCALE 1:1000.

3.2. General Geology of the Klerksdorp Area.

3.2.1. Stratigraphy: The Hartebeestfontein Gold-mine is one of five large producing gold mines situated within an elliptical basin that lies to the east and the south of Klerksdorp (Fig. 1).

The surface consists of dolomite of the Transvaal System which is underlain by Ventersdorp lava over most of the area.

Details of the stratigraphy of the Upper Division of the Witwatersrand System, overlain by a blanket of younger rocks, was obtained from mining operations and bore-holes.

The Upper Witwatersrand beds consist of :-

(a) the Kimberley-Elsburg Series, and

(b) the Main-Bird Series.

The most important auriferous reef in this area is the Vaal Reef which is found at the base of the Bird Reef Stage which forms the top portion of the Main-Bird Series.

The Bird Reef Stage extends from the base of the Vaal Reef to the base of the Kimberley-Elsburg Series, and attains a maximum thickness in the eastern portion of the basin. This stage is subdivided into:-

(i) the Vaal Reef Zone (MB 4 Zone)

(ii) the MB 3 Zone

(iii) the MB 2 Zone

(iv) the MB 1 Zone

(v) the MBA Zone

For the purpose of this investigation, only the Vaal Reef Zone (MB 4 Zone) will be described.

This zone has a fairly constant thickness of 90 feet, at the base of which lies the Vaal Reef. This reef varies from a carbon parting to a well-developed reef more than 4 feet thick. The pebbles are generally small, closely packed, and set in a very pyritic matrix. Carbon is generally present whereas visible gold is rare.

The strata above the Vaal Reef are characterised by the presence of bands of pyritic, small-pebble conglomerates and grits situated at fairly regular intervals. Thin marker-bands are also found at various elevations above the reef, and the quartzite between them is gritty with siliceous and argillaceous partings.

3.2.2. Structure: The greater portion of the area underlain by the Vaal Reef forms an elliptical basin with a north-east to south-west axis. This basin is bounded by the Kromdraai fault in the north-east and the Buffelsdoorn fault in the north-west.

There are two main types of faults :-

(a) Faults parallel to the axis of the basin which are apparently the older. These appear to have had later and renewed movement, and frequently occur in zones or "swarms".

(b) Faults oblique to the axis of the basin are possibly younger as they generally displace the faults mentioned under (a).

Two main groups of intrusives have been distinguished (Wilson, Toens, Oosthuizen, Brink, 1964, pp. 399-416).

3.2.3. Mechanical properties of the rocks in the immediate hanging wall of the Vaal Reef: The rock succession in the immediate vicinity of the Vaal Reef and its properties is given in Table I :

TABLE I

Average Thickness inches	Layer	Slide No.	% Phyllo-silicate	Uniaxial Compressive Strength psi.	Young's Modules x 10^6 psi.
14	C1	-	-	30,000	9.8
0 - 6	AP2	H5	65	19,000	8.8
10	B1	H1, 3, 7	38	28,000	10.1
0 - 1	AP1	H6	65	17,000	9.7
11	A1	HB31	38	27,000	9.4
17	Vaal Reef	HB30	20	-	-
8	A2	H4	45	-	-

The above table shows that there are significant differences in the strengths of the various layers. This variation means that while one layer may still be intact (i.e. the stronger material) an adjoining layer may already be in a fractured state. This could lead to an alteration in the stress field calculated. (This is a very common phenomenon in geology and is the basis of the origin of boudinage structures).

4. GENERAL APPEARANCE AND MEASUREMENT OF FRACTURES IN STOPE 29 S 11 HARTEBEESTFONTEIN GOLD MINE:

The general appearance of fractures in the hanging wall of Stope 29 S 11 is shown in Plates I to III from which it is apparent that they have different orientations with respect to the position of the face. The main parameter is their orientation in respect of the stope geometry and the

appearance of the fracture surfaces. The steps taken to date concerning the orientation and the nature of fractures in the hanging wall of stopes is described below.

4.1. Collection of Data.

A great number of fractures are present in the hanging wall of stopes and, therefore, the rules laid down by Pincus (1951, p.92) in connection with the collection of data on fractures were observed, viz:-

1. Measuring techniques may vary with time as a result of increased efficiency but the body of data collected at a later date may not have a meaning different from that collected earlier.

2. All the data should be collected by the same observer.

3. Major fractures may inadvertently be measured more than once.

4. Variations in the fracture pattern from one sedimentary layer to another must be noted.

The parameters which describe the fracture habit are:-

(a) Dip
(b) Strike
(c) Frequency, and
(d) Surface features.

4.2. Dip of Fractures.

The dip of the fracture planes was measured with the clinometer attached to a Brunton Compass. The accuracy of the readings increased with an increase in the length on dip and a minimum of 2 inches is required. This is exhibited only on strike-brows which means that

measurements are not taken in a straight line over the entire stope span, but in positions wherever such a brow exists. In Stope 29 S 11 they had an average length along strike of 15 feet.

The dip of fractures in Stope 29 S 11 N1 and N2, shown in Figs. 5 and 6 are expressed in terms of distance from the caving line. This line is parallel to the face and marks the face position in the stope where collapse behind the last row of hydraulic props commenced. (The support in the two panels under discussion consisted of skin-to-skin waste-filled skeleton-packs on the raise and strike gulley edges, and four rows of hydraulic props, spaced 4 feet on dip and $2\frac{1}{2}$ to 3 feet on strike. No support was installed behind the fourth row of props, allowing free hanging-wall collapse, or caving, in the worked-out area. The rate of advance of the face is shown in Fig. 3).

The dip of fractures tends to increase with increase in distance from the caving line, equivalent to an increase in stope span. A sudden change in the dip of fractures is closely associated with the caving line.

Although there exists a clear trend, major variations of up to 40 degrees from the average were encountered. This variation does not seem to be a random occurrence, but follows a certain cyclic pattern, as illustrated in Figs. 7 and 8.

Another factor which changes the dip of the fractures is the presence of a locally thicker layer of arenaceous shale (AP 2). Fig. 9 shows that the dip decreases with a decrease in the layer thickness.

PLATE V: Radiating pattern on a Class I fracture surface.

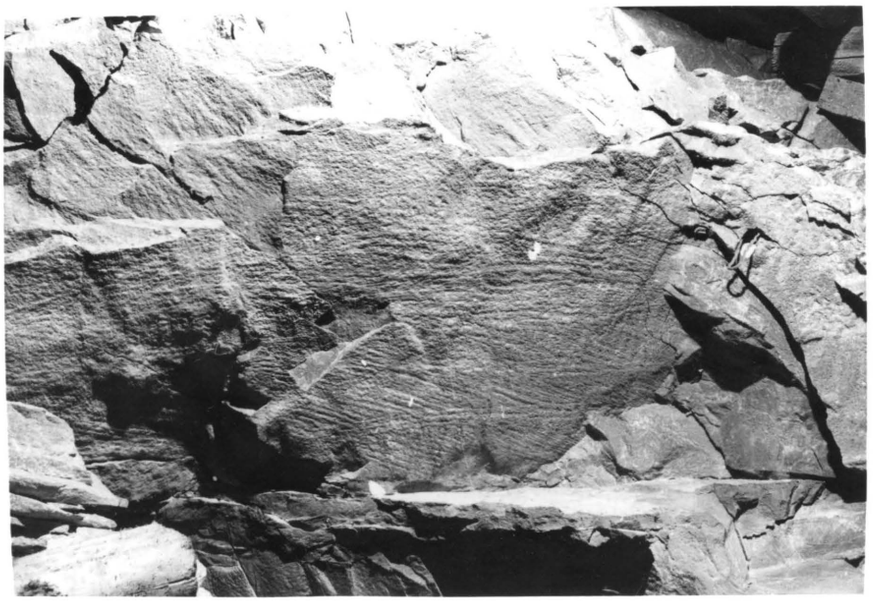

PLATE VI: Cross-bedding on a Class I fracture surface.

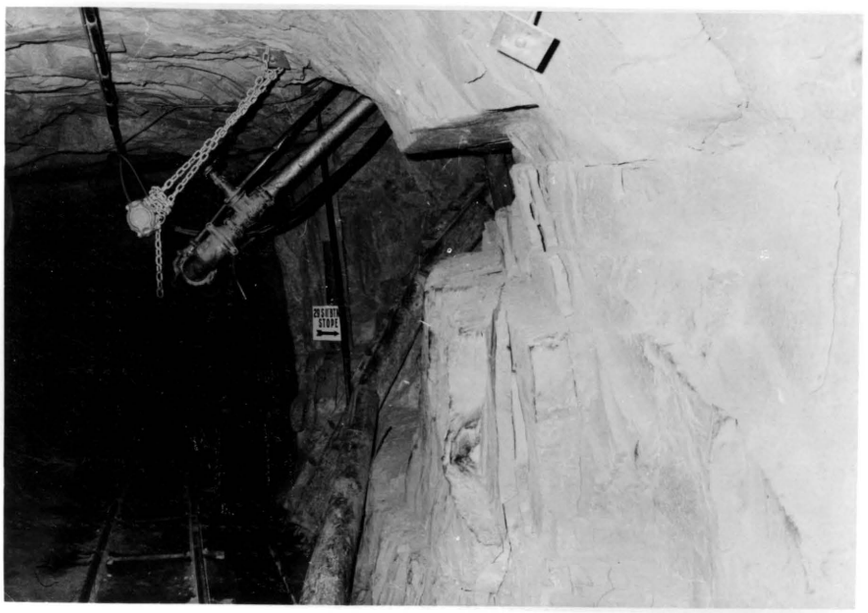

PLATE VII: Class I fracture terminating on bedding planes on the side wall of a tunnel.

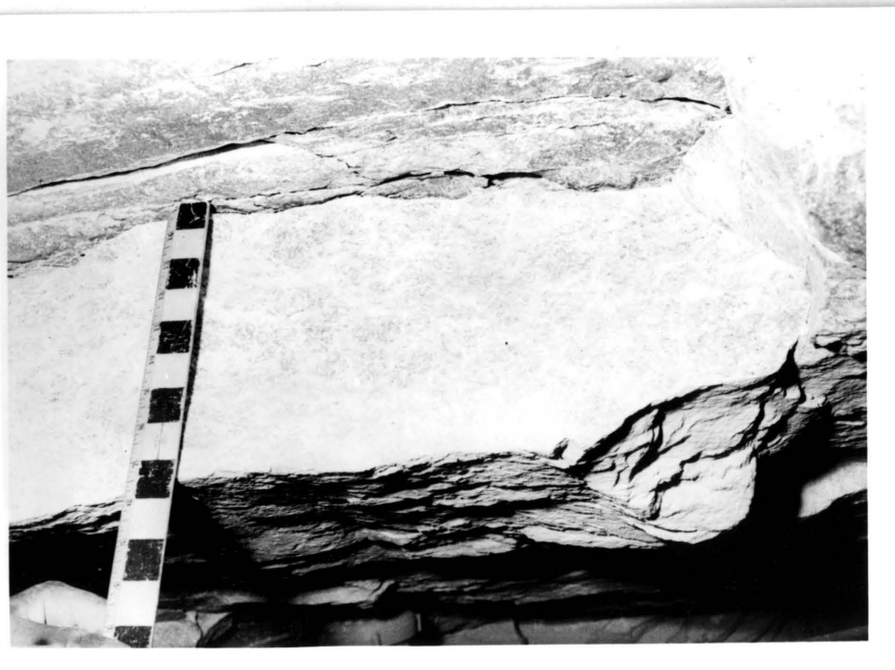

PLATE VIII: Appearance of Class II fracture surface.

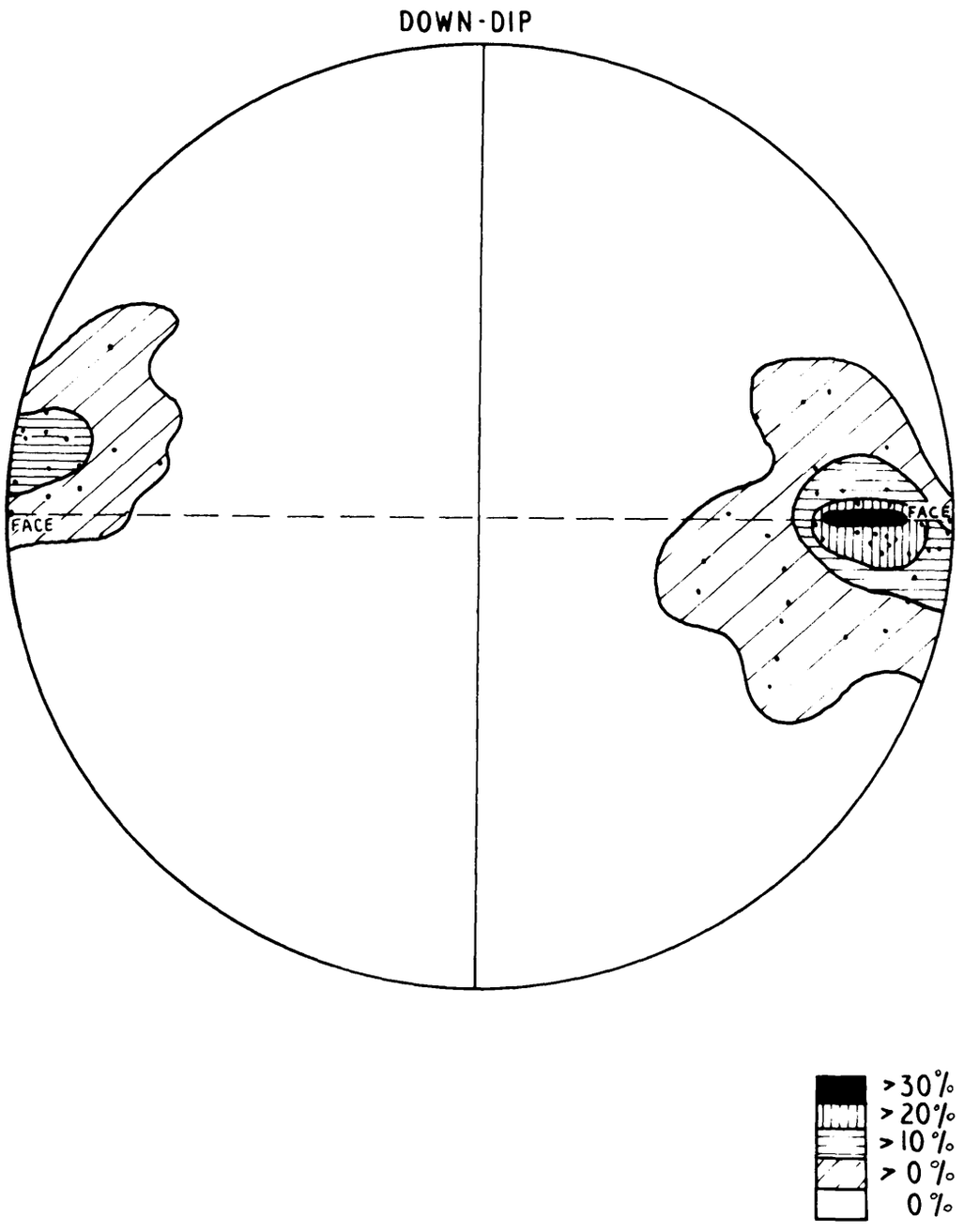

FIGURE 4

SYMMETRY OF FRACTURES IN THE HANGING WALL.

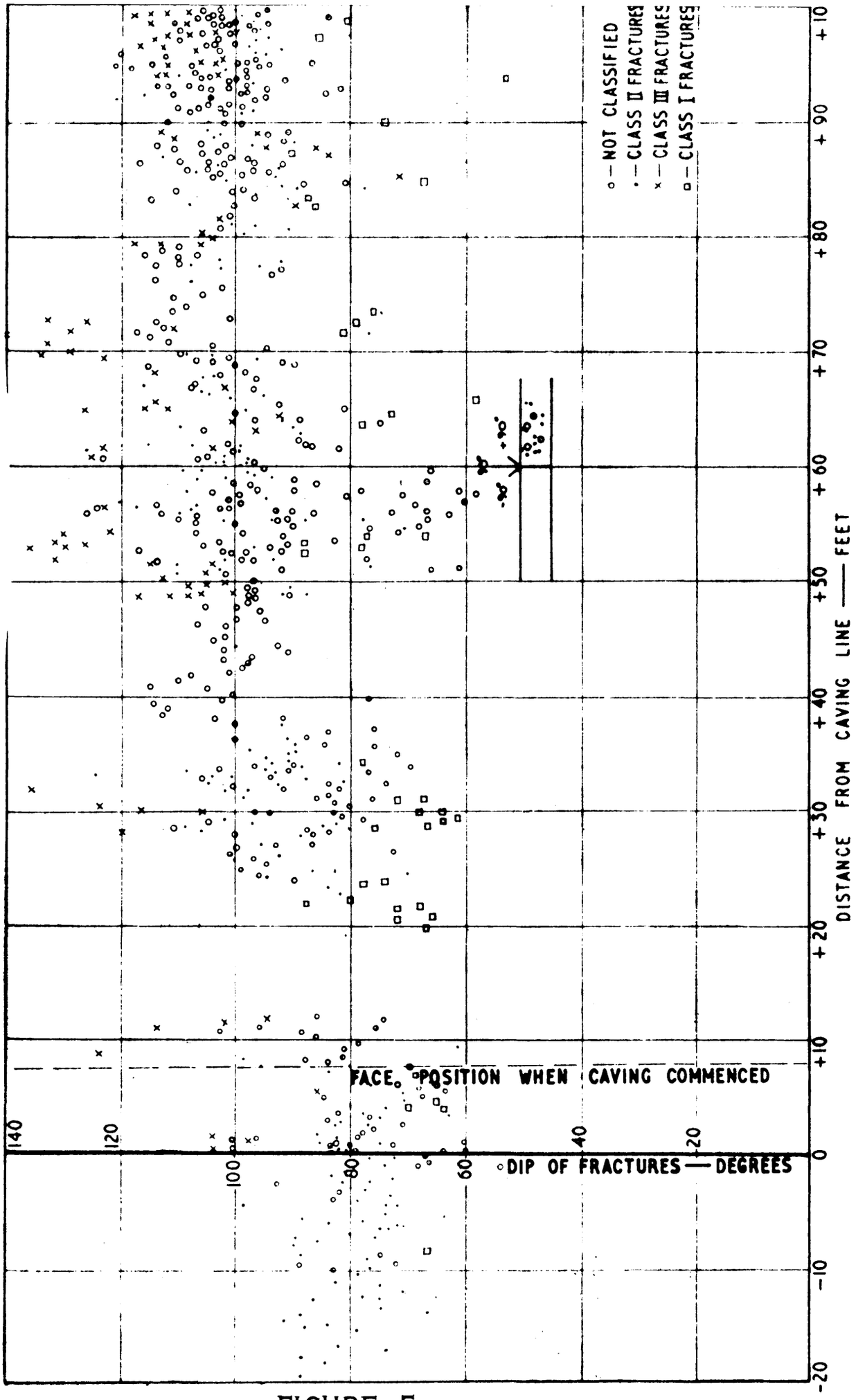

FIGURE 5.

ORIENTATION OF FRACTURES IN 29S11N1 IN TERMS OF DISTANCE FROM THE CAVING LINE

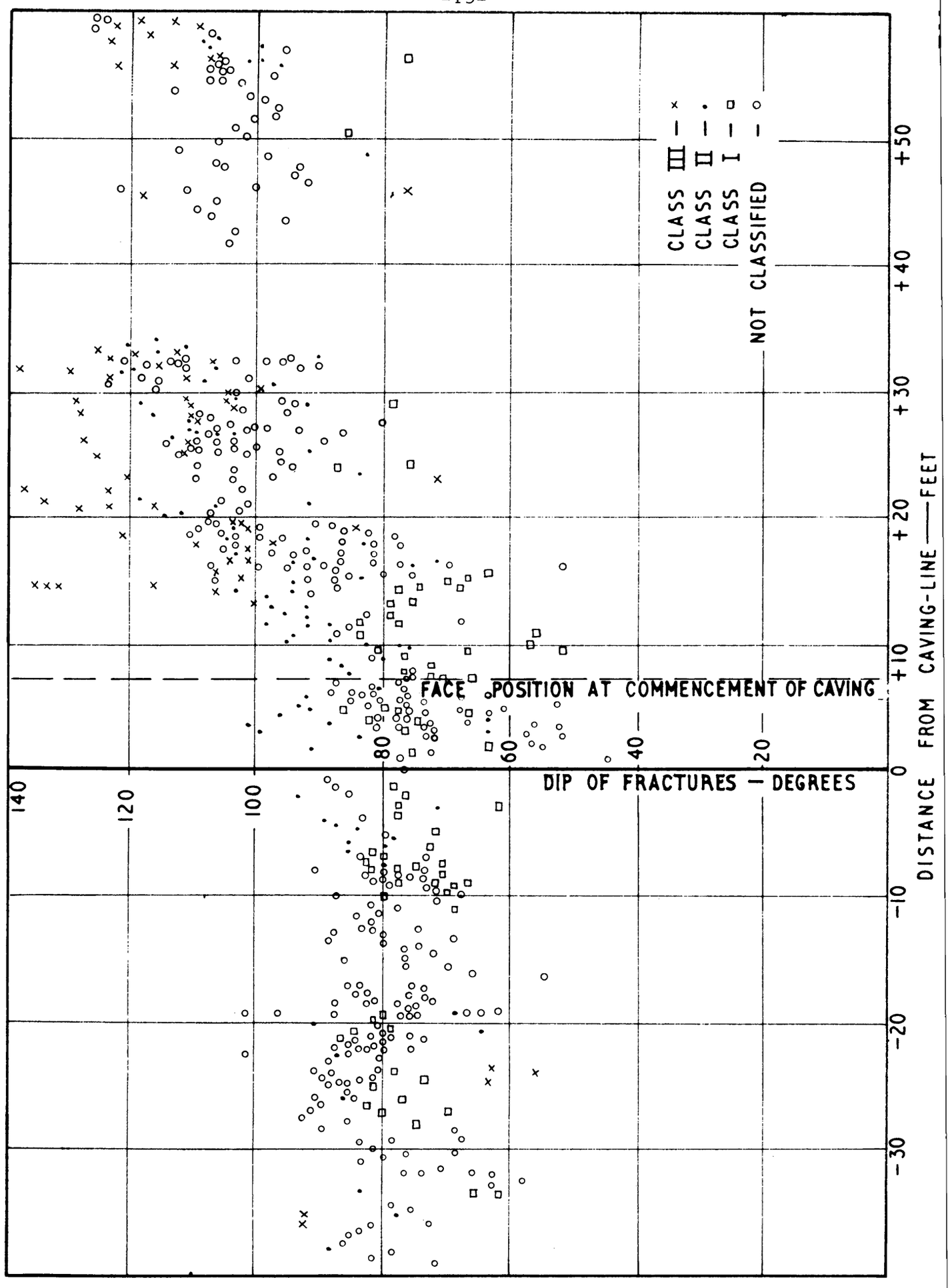

FIGURE 6

ORIENTATION OF FRACTURES IN 29S11N2 IN TERMS OF DISTANCE FROM THE CAVING LINE.

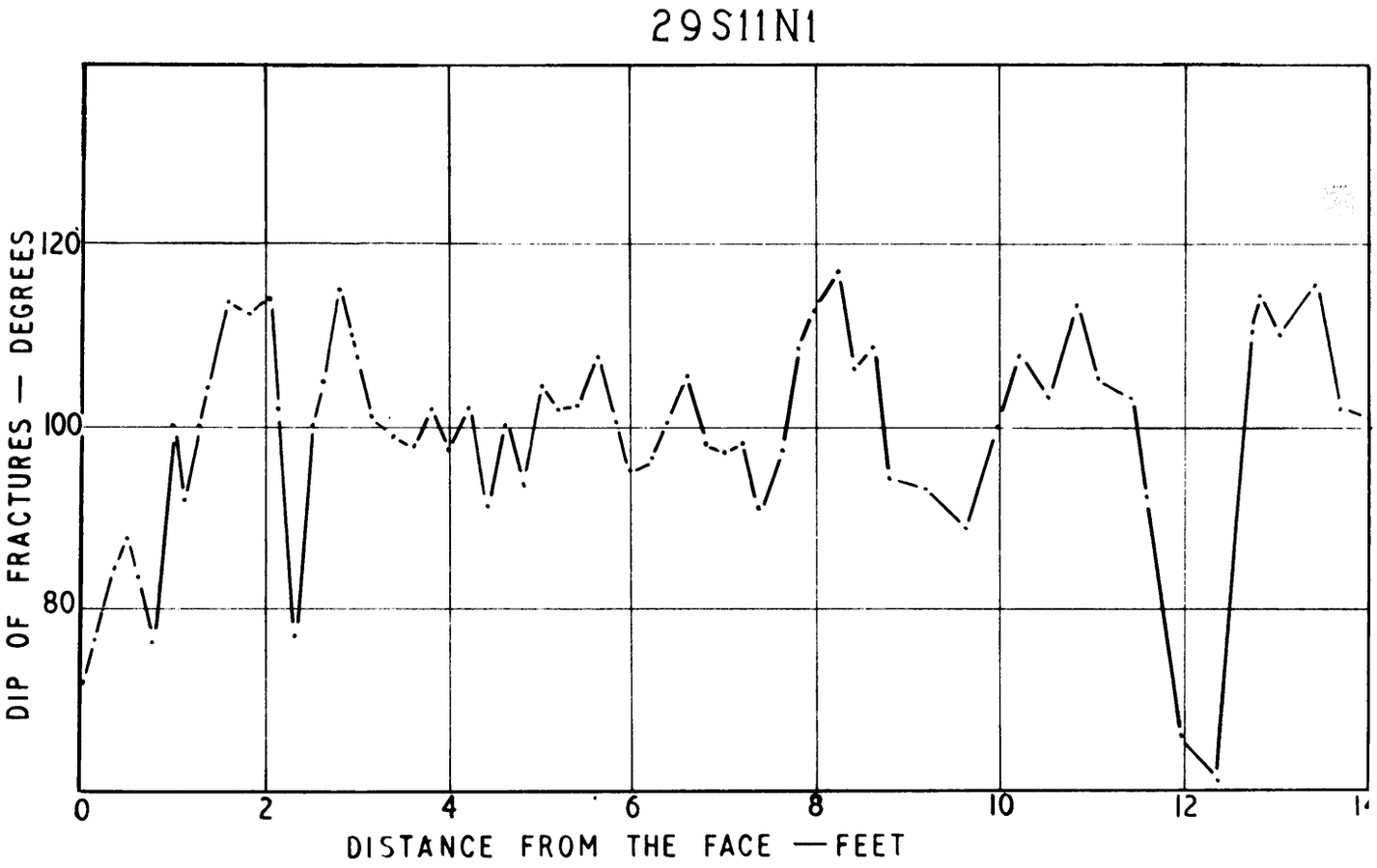

FIGURE 7

CHANGE OF DIP OF FRACTURES IN THE FIRST PANEL HANGING WALL OF 29S11N1.

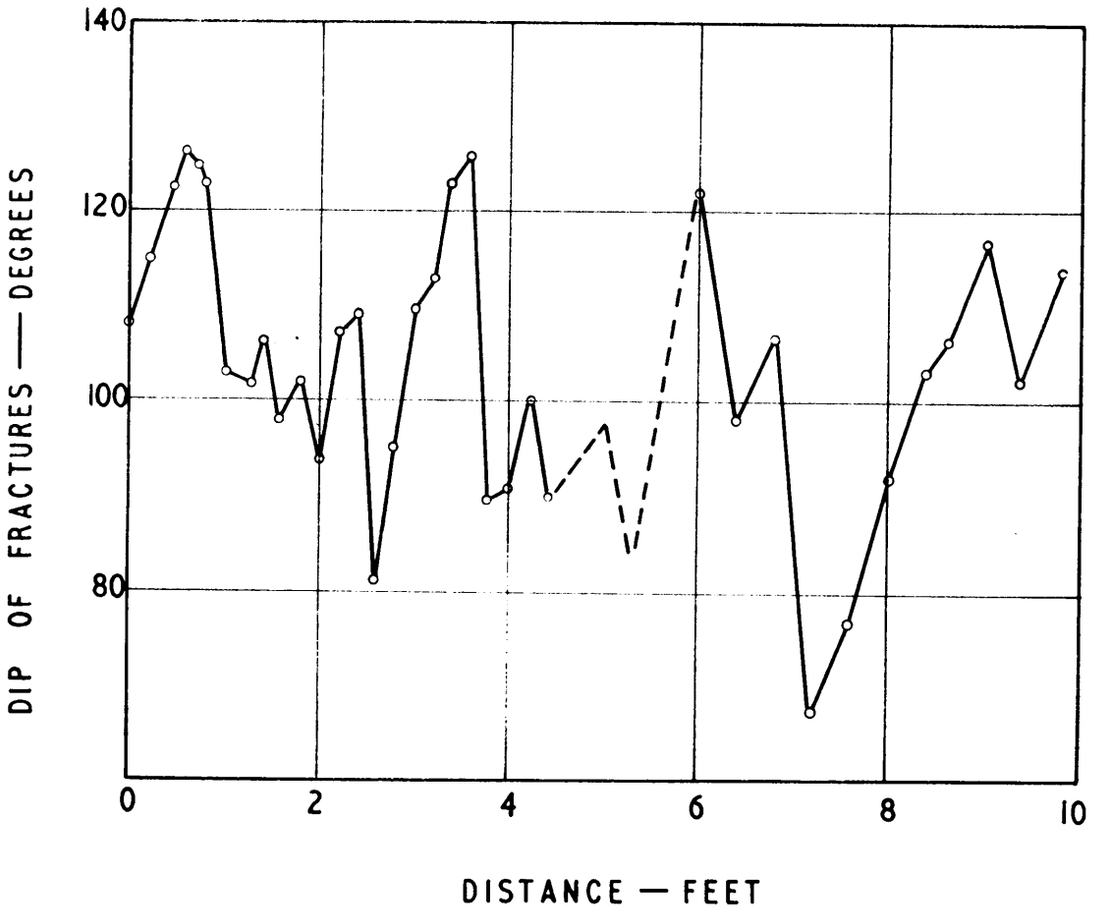

FIGURE 8.

ORIENTATION OF FRACTURES AT A SPAN OF 172 FEET —— STOPE 29S11N1.

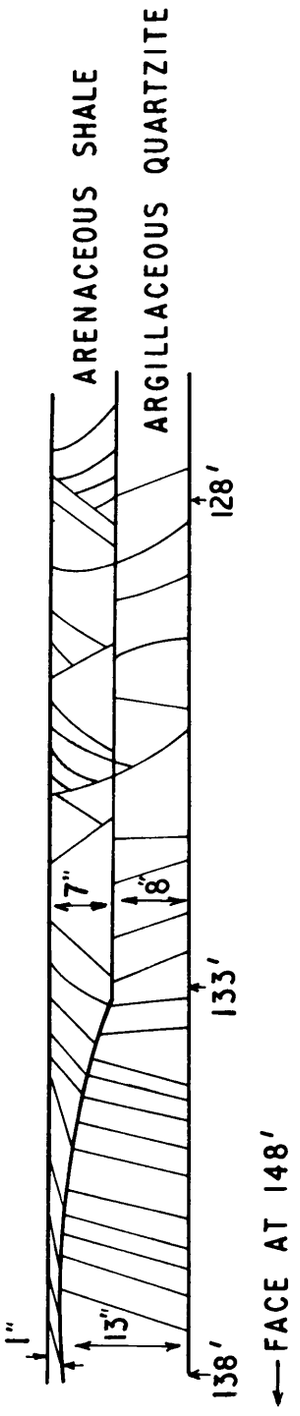

FIGURE 9

INFLUENCE OF DIFFERENT SEDIMENTARY LAYERS ON THE ORIENTATION OF FRACTURES.

of the stope. Two tapes at right angles to the stope face, spaced 5 to 10 feet apart, give the distances of the fracture on dip from the face. These distances can be used to calculate the strike.

4.4. Three-dimensional projection.

The dip and the strike of fractures can be plotted on a Schmidt equal-area net, where the stope face is used as the reference line.

The three-dimensional orientation of some fractures is shown in Fig. 4 on a Schmidt equal-area net with the north-south axis parallel to the stope face. It shows that the strike of the fractures coincides closely with the direction of the face. Therefore, if the direction of the stope face is known and the dip of the fracture plane is given, the orientation of the fracture plane with regard to generally used co-ordinates can be determined. However, since the fractures are related to the stress distribution in front of the stope face, the two-dimensional projection, i.e. dip of fractures only, is given in the following discussion.

4.5. Classification of fractures.

The fractures are classified according to their surface features. Two distinct surfaces can be recognised, with a third type intermediate between these two. It was, therefore, decided to describe the two distinct ones and thereafter give a description of the intermediate type.

4.5.1. Class I Fractures.

Fractures of this class can be distinguished by :-

(a) Fan-shaped linear features with no indications of

movement parallel to the surface. The fracture surface shown in Plate V is often seen in haulages. This represents a good example of Class I fracture surface.

(b) Grain boundaries are distinct and Plate IV attempts to illustrate this.

(c) The fracture line is seldom straight if a length of less than $\frac{1}{2}$ inch is considered. Small undulations and jaggedness are caused by grain boundaries or sedimentary features, e.g. cross-bedding, shown in Plate VI.

(d) The fracture usually terminates against pronounced bedding planes. (Plate VII).

The surfaces of this class coincide with those of fractures which are created by pure tension in the laboratory.

4.5.2. Class III Fractures.

(a) Linear features are the most distinguishing parameter.

(b) The surface is generally covered with powdered material which is geometrically related to the linear features.

(c) The fracture surface may be straight or concave/convex, and is always smooth.

(d) Fractures of this class usually cut across pronounced bedding planes. This applies only where there is no major difference in the strength of the two layers.

The nature of the fracture surface indicates that movement parallel to it has taken place either during or after formation. Such surfaces are found in specimens in which the fracture is not parallel to the direction of maximum principal stress. According to Griggs (1935, p 123), they are shear-fractures.

4.5.3. Class II Fractures.

The surface features of this class fall between those of Classes I and III, and may resemble either. (Plates VIII and IX).

Class I fractures show no signs to indicate movement parallel to the fracture surface, fractures of Class III are distinguished by the clear proof of such movement and Class II fractures are intermediate. Movement parallel to a fracture surface belonging to Class I could take place subsequent to its formation and a fracture surface similar to that of Class II could result. With an increase in movement even a fracture of Class III could be formed from a fracture plane of Class I. Because of this possibility the classification outlined above has been adopted and the terms tension- and shear-fractures will not be used until later in the discussion.

The fractures measured in panels N1 and N2 were not all classified according to the above rules because the surface features could not always be distinguished. After the

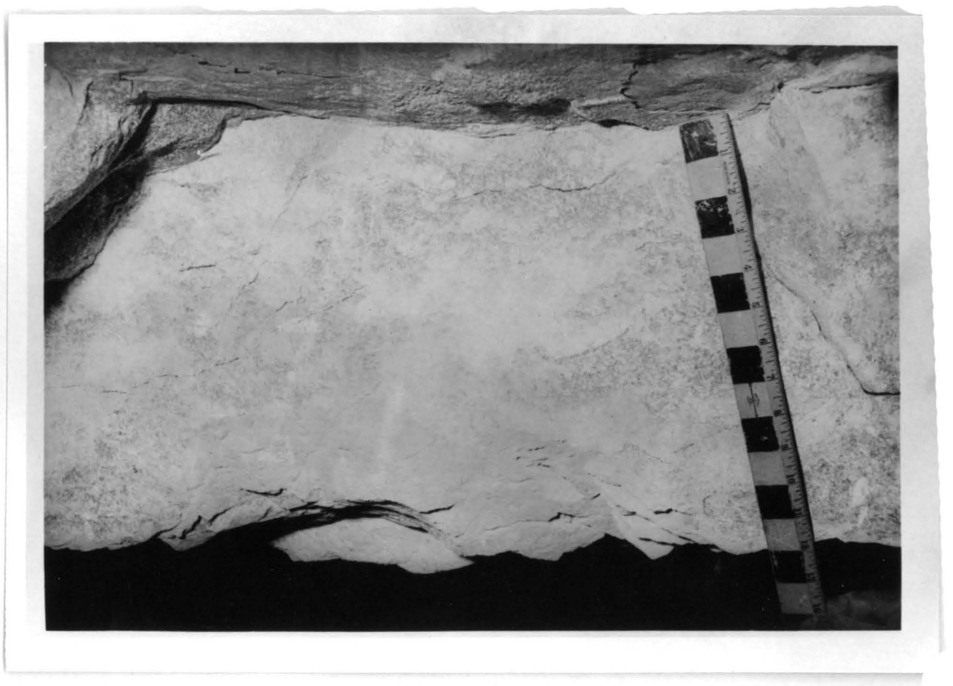

PLATE IX: Appearance of Class II fracture surface.

blast these fracture surfaces are covered by a thick layer of dust and if washed down, some of the diagnostic features, such as the dust created by the movement, disappears. However, some of the fractures could be classified, and these are shown in Figs. 5 and 6.

4.6. Frequency of fractures.

The frequency is the number of fractures over a strike distance of one foot.

Price (1959 pp 16-163) states that frequency of fractures is related to the strain energy stored in the rock and can be used as an indirect check on the stress distribution calculated.

The frequencies measured in layers A1 and B1 are given in terms of the caving line in Figs. 10 and 11 for panels N1 and N2. No obvious difference exists between the frequencies of layer A1 and B1 for the two panels.

It was thought that layer thickness could influence the frequency, but Fig. 12 shows that there is not much relationship over the range of layer thickness measured.

5. METHODS AVAILABLE FOR ANALYSIS:

5.1. Stress distribution around a stope.

Considering a cubic foot of rock at the experimental site prior to any mining, the weight an area of one square foot has to support depends on the densities and thicknesses of the overlying strata.

Three distinct geological formations are present above the points considered :-

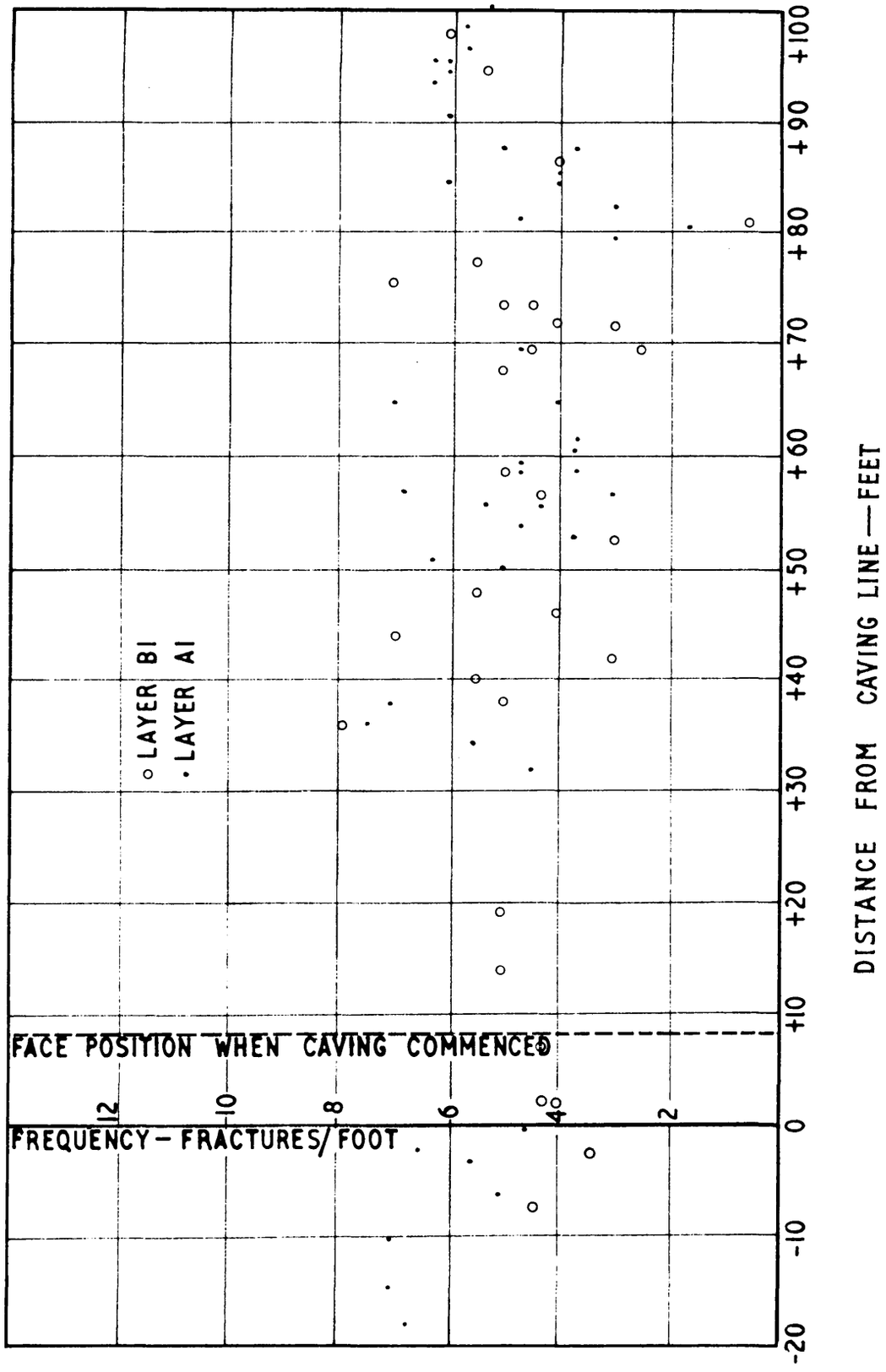

FIGURE 10

FREQUENCY OF FRACTURES IN LAYERS A AND B, IN TERMS OF DISTANCE FROM THE CAVING LINE - 29S11N1.

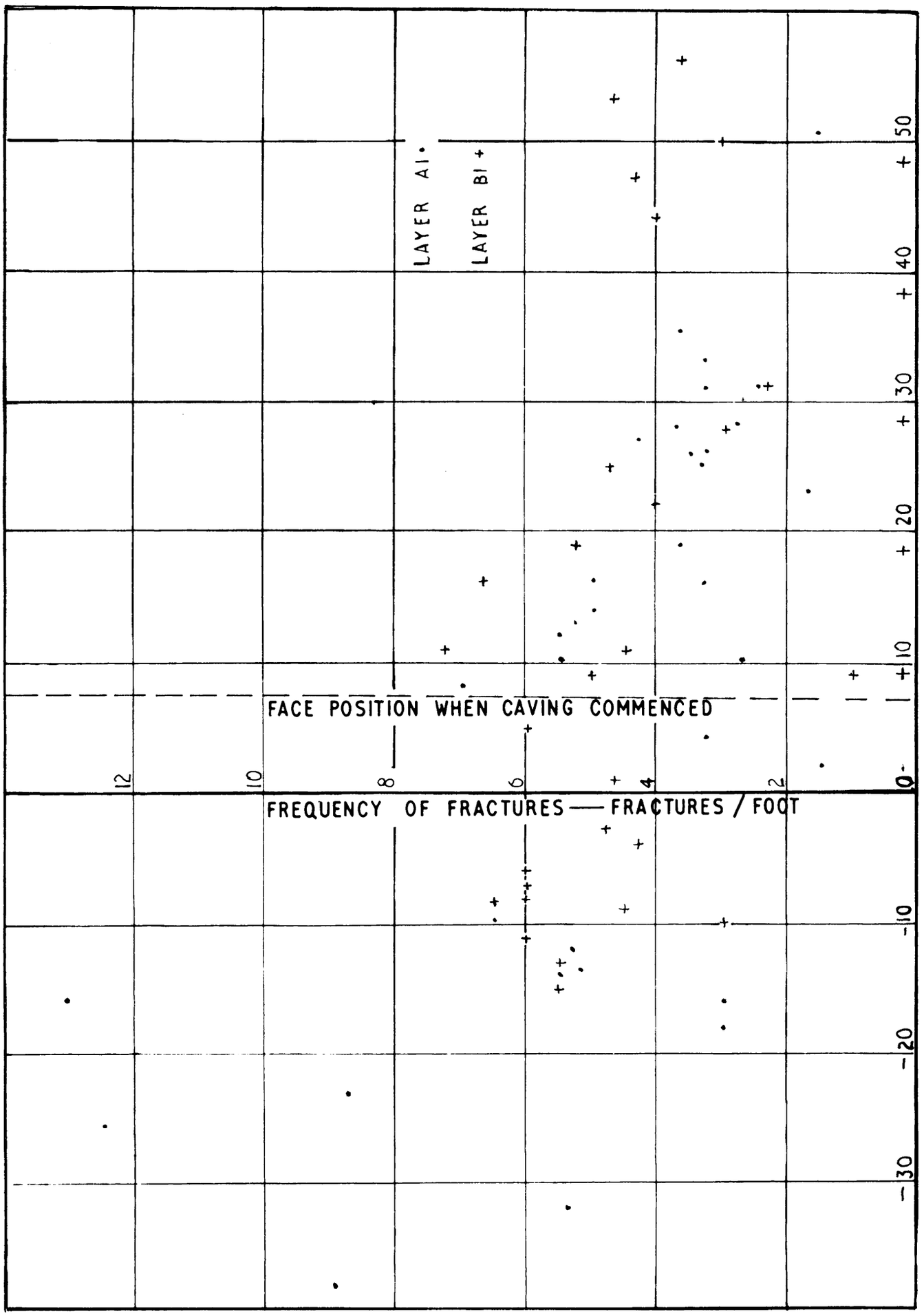

FIGURE 11

FREQUENCY OF FRACTURES IN LAYERS 'A' AND 'B', IN TERMS OF DISTANCE FROM THE CAVING LINE.

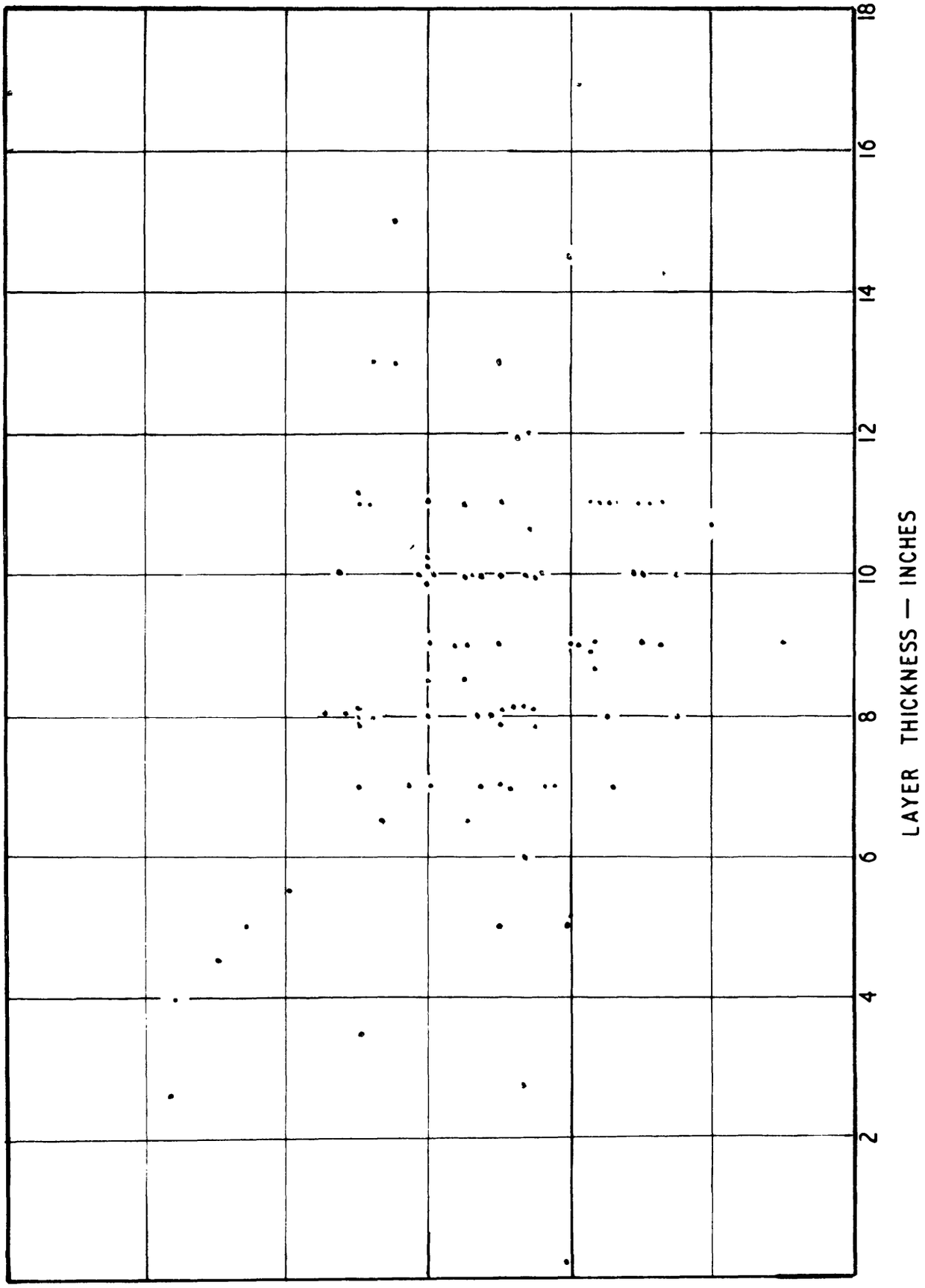

FIGURE 12

RELATIONSHIP BETWEEN THICKNESS OF A LAYER AND THE FREQUENCY OF THE FRACTURES.

Dolomite (Transvaal System)	1,670 feet
Lava (Ventersdorp System)	2,450 "
Quartzite (Kimberley-Elsburg Series)	2,280 "
	6,400 "

The densities of these rocks are 160, 175 and 166.5 pounds per cubic foot respectively. The weight of a column of rock one square foot in cross-section is therefore -

$$(1670 \times 160) + (2450 \times 175) + (2280 \times 166.5) \text{ lbs./ft.}^2$$

$$= 267{,}200 + 428{,}750 + 373{,}620 \text{ lbs./ft.}^2$$

$$= 1{,}069{,}570 \text{ lbs./ft.}^2$$

A quartzite subjected to a load of approximately 500 tons, will tend to expand laterally but since this expansion does not occur, there must be a horizontal force equal and opposite to this attempted expansion. An expression for this is -

$$F_h = \frac{F_v}{(\nu - 1)} \qquad - - - - - - (1).$$

(Mohr, 1963, p.41)

where F_h - horizontal stress

F_v - vertical stress

ν - Poisson's ratio.

The Poisson's ratio for the quartzites at the experimental site was determined in the laboratory and amounts to 0.16.

Substituting this value in equation 1, horizontal force required to maintain equilibrium is found to be 203,218 lbs./ft.^{2}.

The figures given above are unwieldy and for this reason pounds per square inch (p.s.i.) is used in practice. This requires a division by 144 and the figures become 7,466.2 p.s.i. and 1,866.6 p.s.i. respectively for the vertical and horizontal stresses.

The vertical and horizontal stresses coincide with the principal stress directions and are therefore maximum and minimum principal stresses. (A principal stress is in the direction in which the shear stress is zero).

The equilibrium referred to above will be disturbed as soon as mining commences. If one cubic foot of rock is mined, the load originally carried by the mass of rock will be transferred to the adjacent rock, thereby increasing the load per unit area next to the excavation. The load remains the same but the stress increases because the supporting area decreases. It is clear that in order to maintain equilibrium, a complete change in the stress distribution must take place.

The change in a stress field as a result of excavations can be calculated according to methods described in textbooks dealing with the theory of elasticity and the method used is that proposed by Savin (1961). The staff of the Rock Mechanics Division of the Council for Scientific and Industrial Research (C.S.I.R.) at Pretoria has developed this method further (1965) and the stress distribution in two dimensions in the immediate vicinity of an elongated slit can now be calculated. Since this is equivalent to a section along a stope on strike it is possible to obtain stress values in the immediate vicinity of the stope face where it is assumed that

the fractures measured have originated.

The maximum principal stresses at different distances ahead of the face and for different stope spans are given in Fig. 13.

The minimum principal stress is expressed as a ratio of the maximum principal stress, the k-ratio, in Fig. 14.

Fig. 15 gives the orientation of the maximum principal stress at different distances ahead of the stope face for various stope spans.

5.1.1. Discussion of assumptions made in the theoretical model.

The basic assumptions made are that :-

(a) the theoretical model is an elongated ellipse approximating the outline of a stope on strike.

(b) the material in which this two-dimensional slit is situated is a completely homogeneous, isotropic, elastic medium, and

(c) the calculations are based on individual spans of 40, 80, 120, 160 and 200 feet; it disregards the possibility of fracturing over the spans covered.

Plate I shows that the intersection of the hanging wall with the stope face is a sharp corner. From the theory of elasticity it is known that stresses at such a corner must become infitely high (Jaeger, 1964, p.191) and therefore the quartzite should fail. The explanation for Plate I must therefore be that the material in front of the face must be slightly fractured, and that the stress distribution in

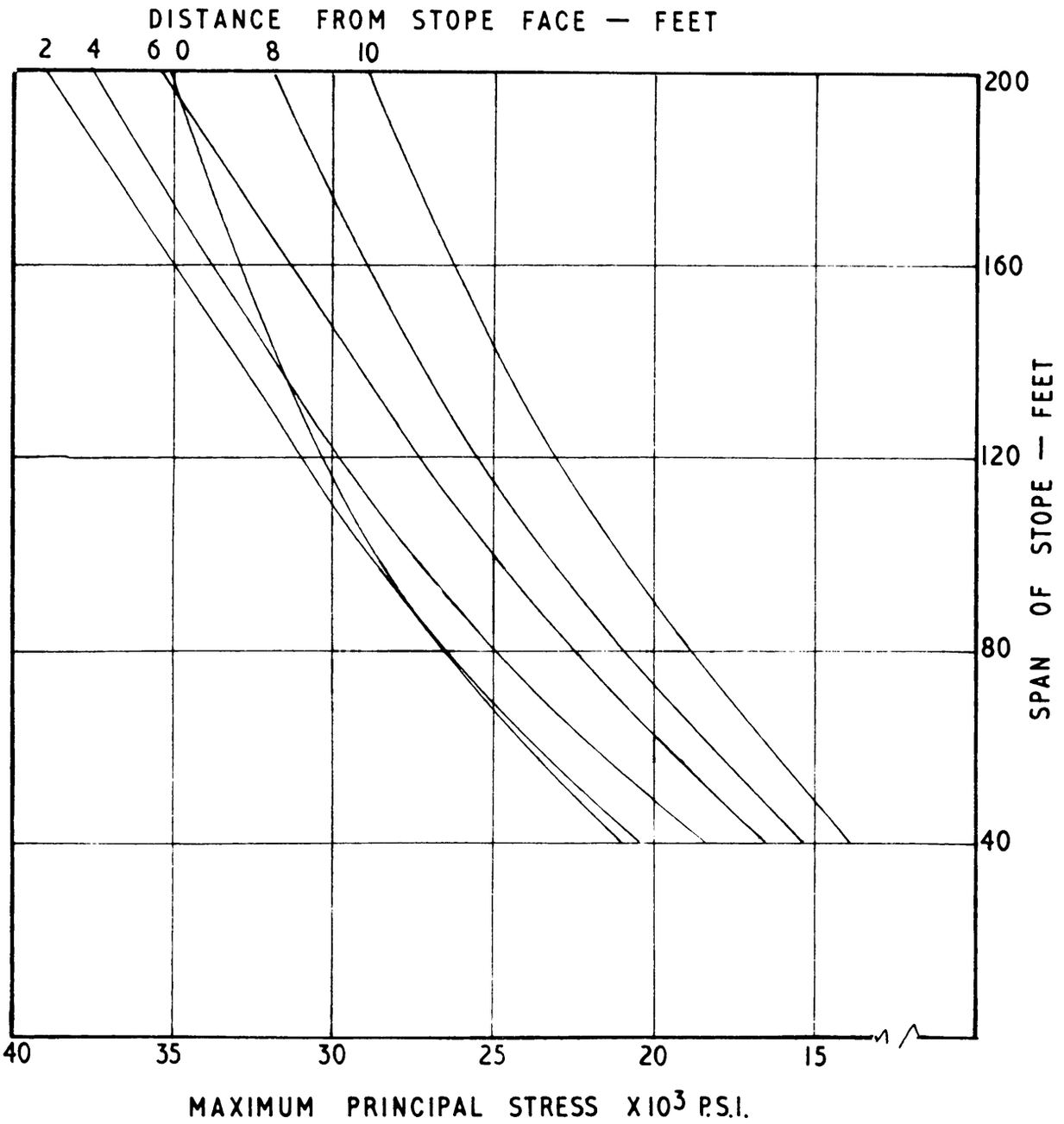

FIGURE 13

MAXIMUM PRINCIPAL STRESS AT VARIOUS DISTANCES AHEAD OF A STOPE FACE — 6400 FEET BELOW SURFACE.

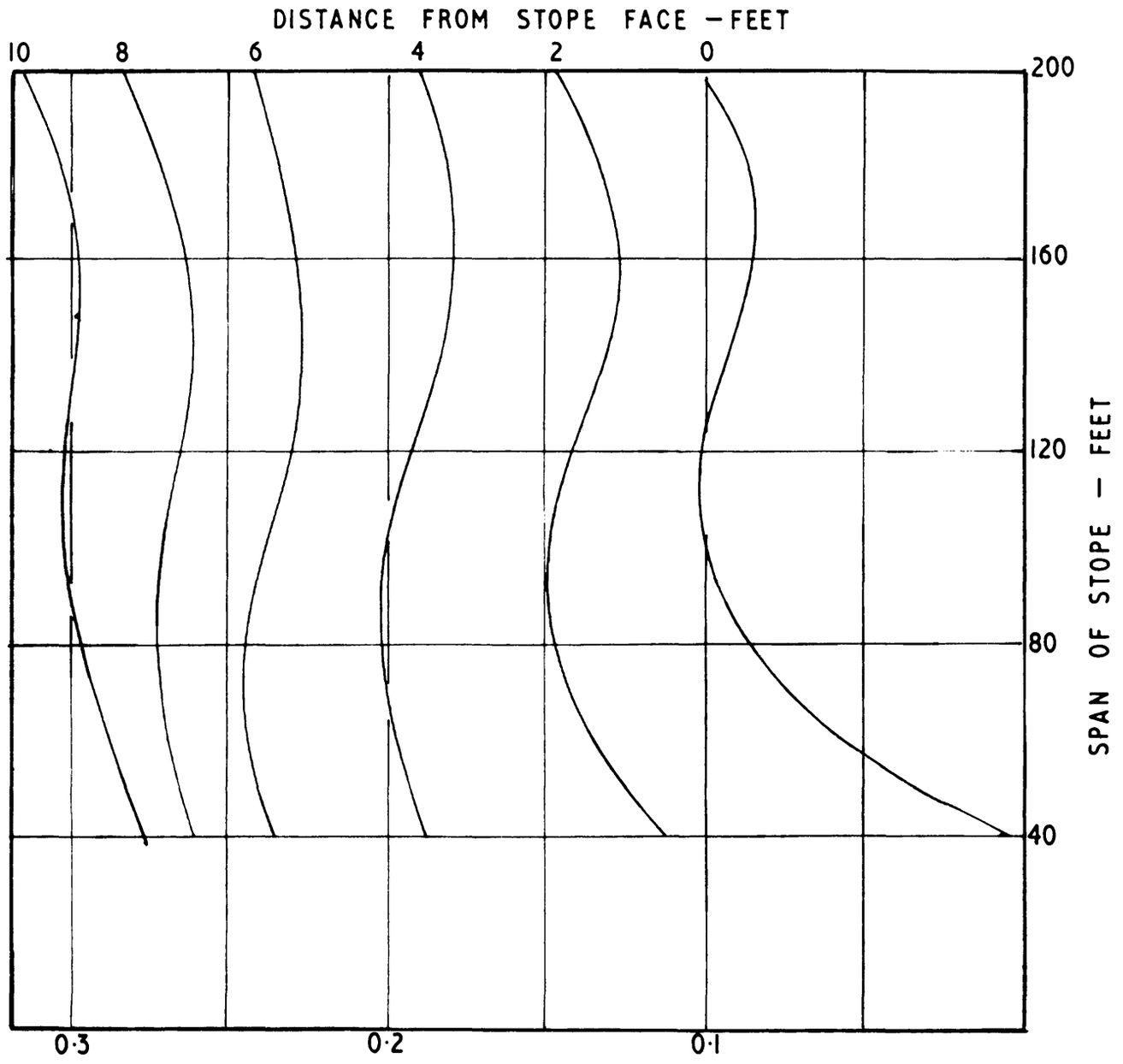

$$\text{K-RATIO} = \frac{\text{MINIMUM PRINCIPAL STRESS}}{\text{MAXIMUM PRINCIPAL STRESS}} = \sigma_3/\sigma_1$$

FIGURE 14

CHANGE IN K-RATIO WITH INCREASE IN THE SPAN OF A STOPE.

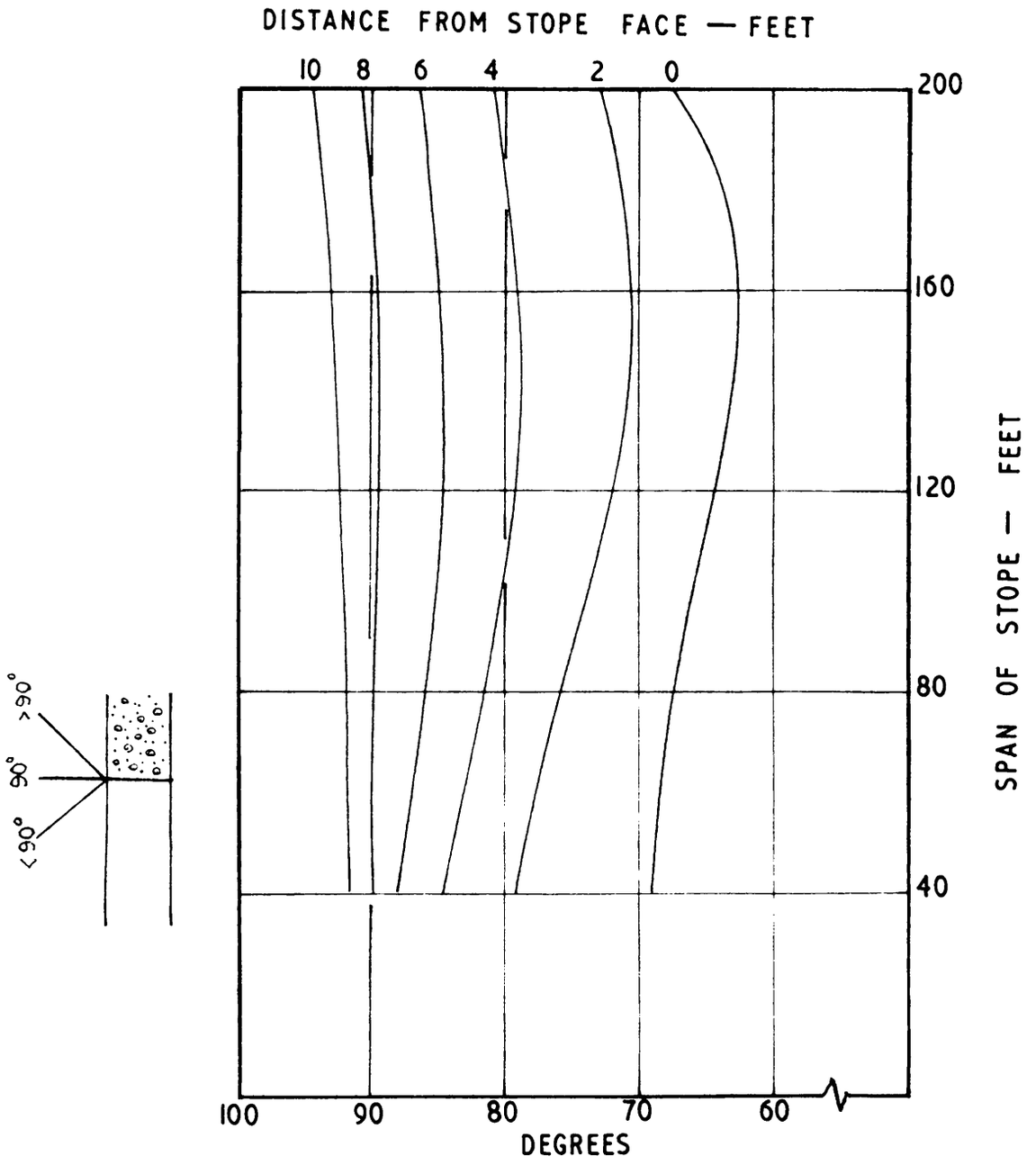

FIGURE 15

ORIENTATION OF THE MAXIMUM PRINCIPAL STRESS AT VARIOUS DISTANCES AHEAD OF THE STOPE FACE.

actual fact follows the rounded corners of the elliptical shape assumed.

Fig. 3 shows that the stope is not very long in the direction of dip and therefore the two-dimensional assumption is not completely valid.

It was shown (Ryder and Officer, 1965, p.187) that a two-dimensional treatment does not give exact results, but the influence of this did not invalidate the comparison between predicted and measured values. In the present discussion it is assumed that the influence of the third dimension is very slight near the centre (dip direction) and in the immediate vicinity of the stope face.

The assumption of homogeneity, isotropy and elasticity is applicable in a case such as investigated by Ryder and Officer (1965, p.183) but in the present case where the layer thickness is of the order of the field investigated, it is incorrect to assume that the material is homogeneous. Table I shows this, as well as the sketch in Fig. 9.

Individual pieces of this quartzite behave in an elastic manner and it is assumed that the succession given in Table I could behave as such, with the exception of AP1 and AP2 which are argillaceous partings and show definite time-dependent properties (C.S.I.R., 1963).

The individual layers could well be isotropic but the sequence as a unit could show anisotropic characteristics.

The homogeneity and possibly the anistropy of the rocks could therefore influence the distribution of stresses in the actual underground condition. This cannot be included in this theoretical model.

Observations underground show that fractures appeared in the hanging wall at a stope span of approximately 100 feet. However, the theoretical model is based on the assumption that the material around the ellipse is solid for all spans calculated.

The factors discussed above will influence the predicted stress distribution to a certain degree, the extent of which could be estimated by the divergence between predicted and measured values.

5.2. Failure Criteria.

A failure criterion simply provides a formula which permits the prediction of the strength of a material under any state of multiaxial stress, based upon a critical quantity which may be determined in one type of test, for example the uniaxial tensile or compression strength test. (Bieniawski, 1966, p.1).

5.2.1. The Strain Ellipsoid.

Strain is the only measurable quantity and therefore it is natural to set up a fracture criterion in terms of strain, rather than of stress, and the strain ellipsoid could possibly be used for this purpose.

An attempt in this direction was made by Becker (1893, p.71) in which he assumed that fracture planes will lie in the plane of the circular cross-section where the shearing strain is a maximum.

This assumption can be illustrated by means of a wire-netting experiment (Bucher, 1921, p.14). The outstanding characteristics of this experiment is that the elongation in the direction

of one principal stress equals the shortening in the direction of the other principal stress. This implies that the area of the strained surface remains unchanged.

The criterion was used extensively for many years (Jaeger, 1964, p.86, Swanson, 1927, p.193). Experiments by Bucher (1921,p.14), Griggs (1935,p.126), Kahlbaum and Seidler, and Lea and Thomas (Griggs, 1935, p.126), proved that the strain ellipsoid cannot be used as a fracture criterion. Leith (1937,p.368) states that it is useful as a standard of comparison between different structures - a purely geometrical aid for comparative purposes (Turner and Weiss, 1963,p.268).

As this is the only criterion which is based on the strain of materials, the remaining criteria are expressed in terms of stress.

5.2.2. Mohr's theory of fracture.

The fundamental postulate of this theory is (Bucher, 1921,p.7) -

> "The ultimate strength of the material is determined by the greatest shearing stress (τ) in the shearing planes; this limiting shear itself depending upon the normal stress in the planes. The limiting shear is assumed to be some function of the normal stress (σ) in the plane $\tau_m = f(\sigma_n)$
>
> σ_n = normal stress."

This theory can be expressed in a graphical form for which Bucher (1921,pp.1-6) gives formal approval.

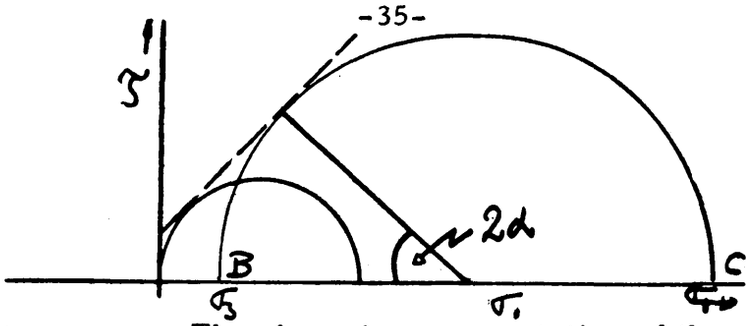

The above is a presentation of the stress distribution in a material which is subjected to a biaxial stress field. The circle BC gives the minimum (σ_3) and maximum (σ_1) stress values at the stage when the material fails. With an increase in the lateral compression, there is an increase in the strength of the material and hence an increase in the slope of the curve known as the Mohr envelope which is characteristic of different materials and represents the relation -

$$\tau_m = f(\sigma_n)$$

This curve has to be determined experimentally for different rock types. The failure point is determined by a change in the maximum (σ_1) and minimum (σ_3) stresses and the value of σ_1 and σ_3 where failure occurs are then plotted on the normal stress axis and a circle with $\frac{\sigma_1+\sigma_3}{2}$ as centre point with a radius of $\frac{\sigma_1+\sigma_3}{2} - \sigma_1$ is then drawn.

The following additional information is obtained from the Mohr envelope :-

1. Since the envelope is completely determined by sets of the maximum and minimum principal stresses at failure the strength of a material must be entirely independent of the intermediate principal stress.

(Recent information (Wiebols and Cook, 1968,p.530) sugge that the value of the intermediate principal stress has a powerful and

regular effect on the strength of rock. However, in the modified Griffith criterion this effect cannot be accounted for and will, therefore, not be dealt with in the present paper).

2. The angle 2α gives the value of the angle between the two conjugate shear planes. (Bucher, 1921, p.7). Experiments have shown that the envelopes are roughly parabolic in shape. This implies that with increase in lateral compression the strength increases, and the value of 2α increases and approaches 90 degrees. The material therefore becomes more plastic (ductile) with increasing lateral confinement, or alternatively, with lateral tensions the material becomes more brittle. These statements have been borne out by experience (Bucher, 1921, p.13).

5.2.3. <u>The Navier-Coulomb criterion of failure.</u>

According to Anderson (1951, p.3) this failure criterion can probably be assigned to Coulomb. He states that the rock will fail along planes at which the shear stress is a maximum. In a biaxial stress field, the shear stress, and the stress normal to these planes, can be calculated by means of the formulae.

$$\tau = \frac{\sigma_1 - \sigma_3}{2} \sin 2\alpha \quad - - - - (2)$$

$$\sigma_N = \frac{\sigma_1 + \sigma_3}{2} + \frac{\sigma_1 - \sigma_3}{2} \cos 2\alpha \quad - - - (3)$$

Where τ = shear stress on a plane inclined at an angle to the maximum principal stress direction.

σ_N = stress normal to the plane inclined at an angle to the maximum principal stress direction.

σ_1 = Maximum principal stress.

σ_3 = Minimum principal stress.

The value of sin 2α varies between 0 and 1, the latter being attained at sin 90°. This gives the maximum value for $\tau = \frac{\sigma_1 - \sigma_3}{2} \times 1$. According to Coulomb, a material should fail in planes orientated at 45 degrees to the direction of the maximum compression. This happens very seldom. In 1833 Navier introduced a "co-efficient of internal friction" (Anderson 1951, p.4) (μ) which he regarded as being constant for a specific material. This co-efficient has the effect of reducing the angle below a value of 45 degrees.

Equation 3 gives the stress normal to any plane and the higher this stress becomes, the higher the shearing stress must be to induce movement.

This is also expressed by the equation -

$$\tau = \mu \sigma_N$$

where μ is the co-efficient of internal friction, and with an increase in its value, the shear stress must be increased to induce movement.

To produce a discontinuity, the available energy has to overcome the strength of the material and the internal friction which is proportional to the normal pressure across the discontinuity. The shear stress is always greatest in a direction at 45 degrees to the

principal stresses. If the plane is rotated from this position towards the axis of maximum principal stress, both the shear stress, which tends to produce movement, and the normal pressure, which opposes movement, becomes smaller. Depending upon the specific properties of the material, there will be one particular angle (α) for which the combined effect of the two opposing factors becomes most favourable for fracturing to take place (Hafner 1961 p 381).

Anderson (1951, p.10) calculated the orientation of these planes which are given by the formula $\tan 2\alpha = \pm 1/\mu$ This relationship is illustrated in Fig. 19.

5.2.4. The Griffith theory of fracture.

The Navier-Coulomb criterion of fracture can be used to determine the directions of the maximum principal stresses, but it does not explain under what conditions the fractures are formed nor how tension-fractures are created. The Griffith theory attempts to explain the mechanism involved.

Griffith (1920, p 198) states that all solid materials must contain minute cracks distributed at random and that fracturing results by extension of these cracks. This would explain the discrepancy between measured strength and the theoretical strength calculated by considering the molecular cohesion.

The minute cracks have the effect of changing the stress field in their immediate vicinity, and if they are subjected to a specific external stress field, high tensile forces, which can rupture the molecular bonds, are induced at the crack tip.

Griffith simplified his calculations by disregarding the influence of the friction resulting from the closure of cracks.

MacClintock and Walsh (Brace, 1960, p.3478) considered this influence and modified the theory accordingly. The internal frictional resistance will increase with increased compressional forces, and the material will become stronger. This condition is illustrated in Fig. 16 for four values of the coefficient of internal friction.

The increase in strength of the material with increase in compression is such that beyond a certain k-value, the material becomes highly resistant to fracture as shown in Fig. 17.

The relationship between the directions of principal stress and the resulting fracture plane, is a function of the applied stress field and the coefficient of internal friction. By applying a load to a specimen a complex stress field will result around each individual micro-crack and the magnitude of the tensile stress at the tip of the crack will, in a certain orientation, exceed the molecular cohesion.

The orientation of these critical cracks is given in Fig. 18 where it can be seen that for k-ratios less than -0.33 (tensile field) the critical crack is parallel to the maximum principal stress, while for k-ratios in excess of 0.1, the orientation of the critical crack remains constant. This latter value is the same as that predicted by the Navier-Coulomb criterion of failure (Fig. 19).

The modified criterion is based on a failure mechanism proved to be correct by comparison with laboratory tests. (Hoek, 1965, p.135).

This theory may, therefore, be used to calculate a Mohr envelope and the uniaxial compressive strength. (Hoek, 1965, p. 36).

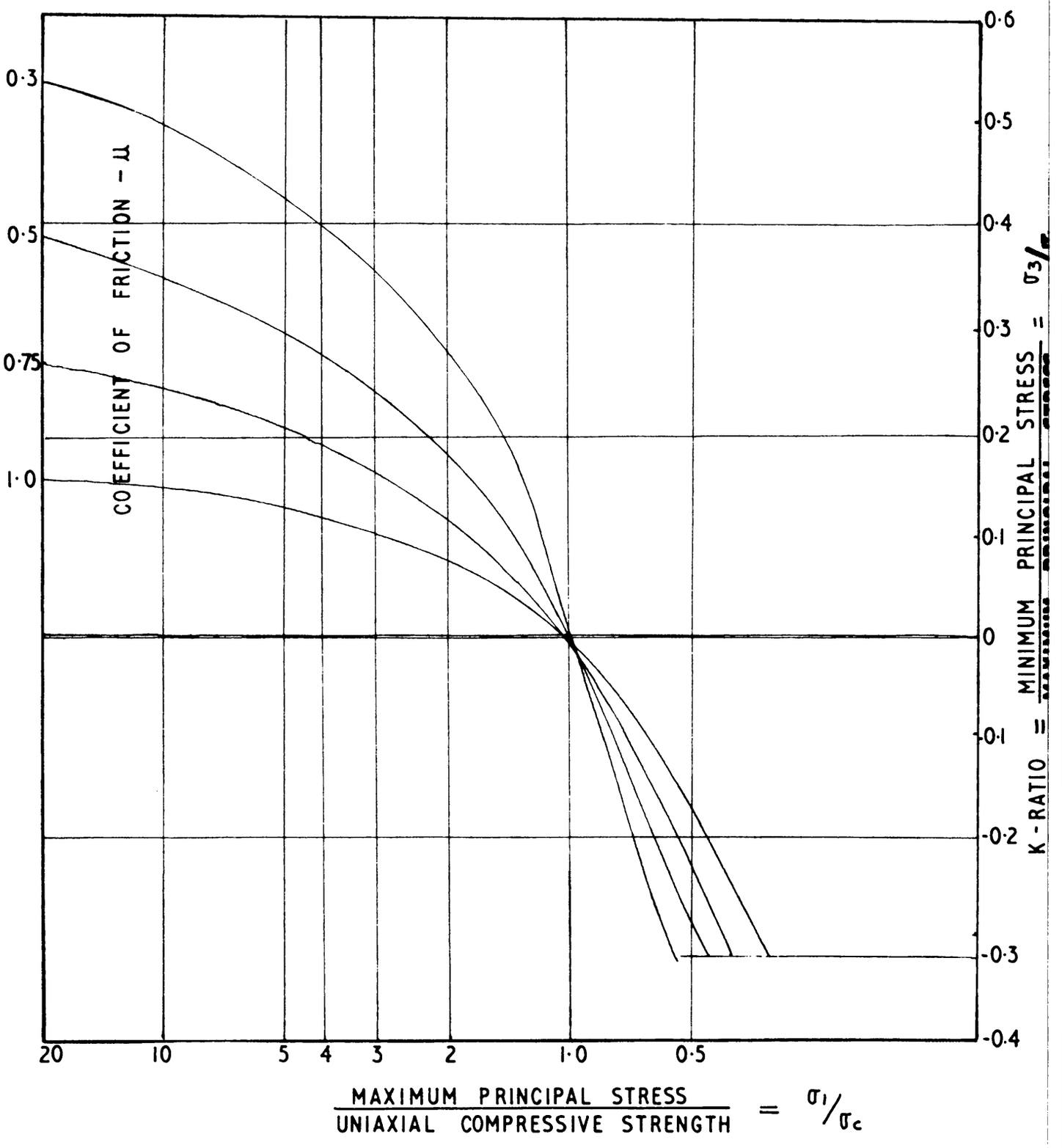

FIGURE 16

CHANGE IN THE FAILURE STRENGTH OF ROCKS WITH DIFFERENT COEFFICIENTS OF INTERNAL FRICTION.

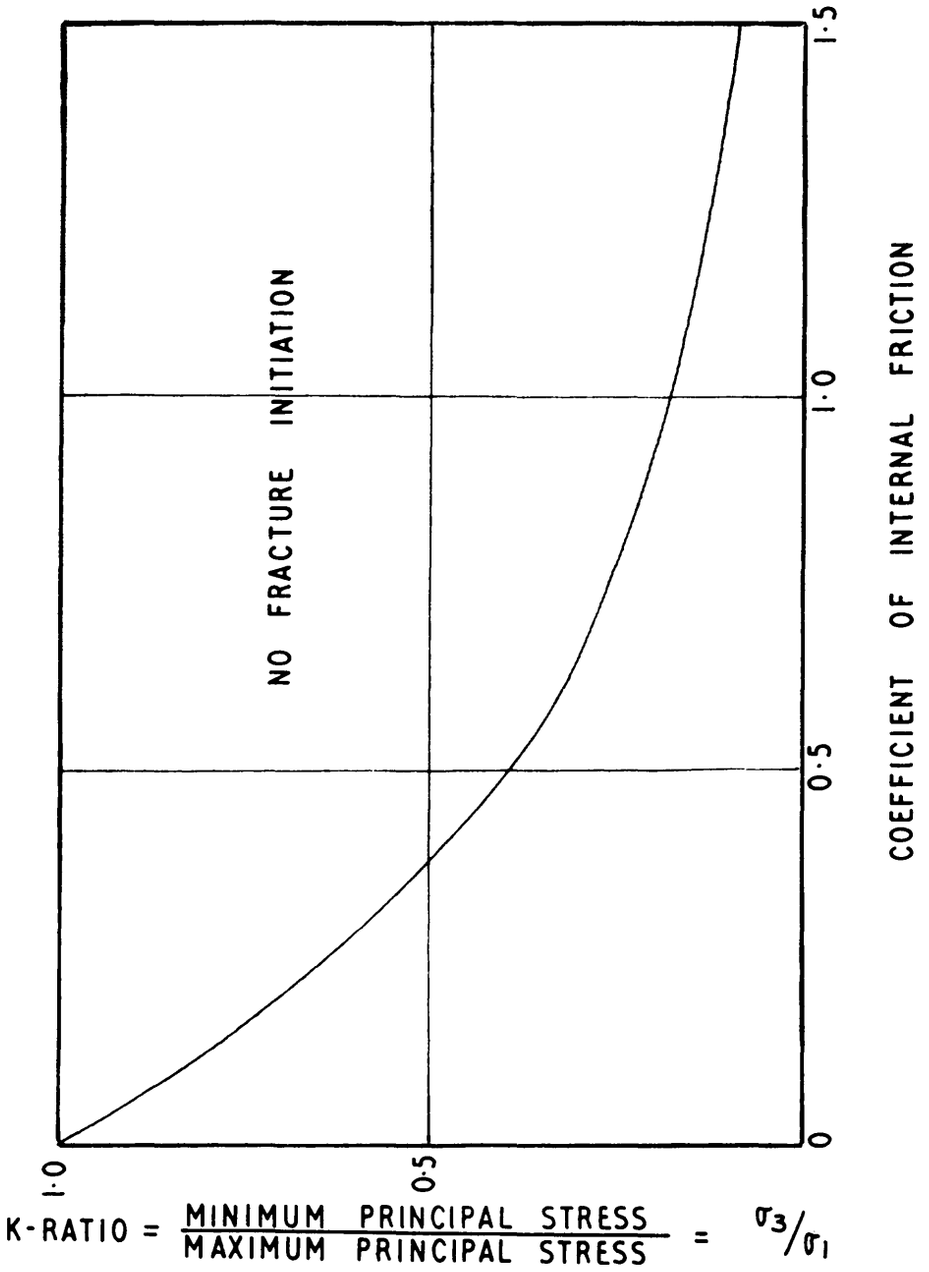

FIGURE 17

LIMIT OF FRACTURE INITIATION FOR VARIOUS COEFFICIENTS OF INTERNAL FRICTION.

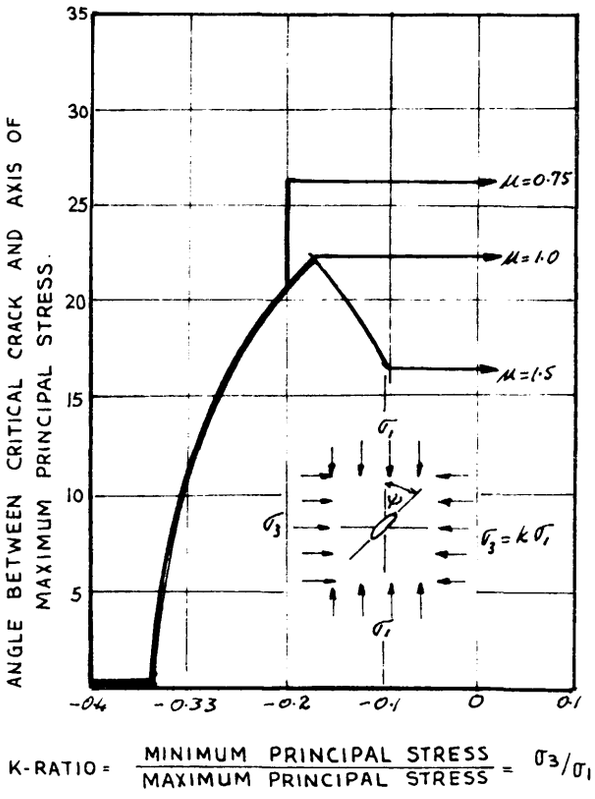

FIGURE 18

CRITICAL CRACK ORIENTATION FOR DIFFERENT K-RATIOS (AFTER E. HOEK 1966)

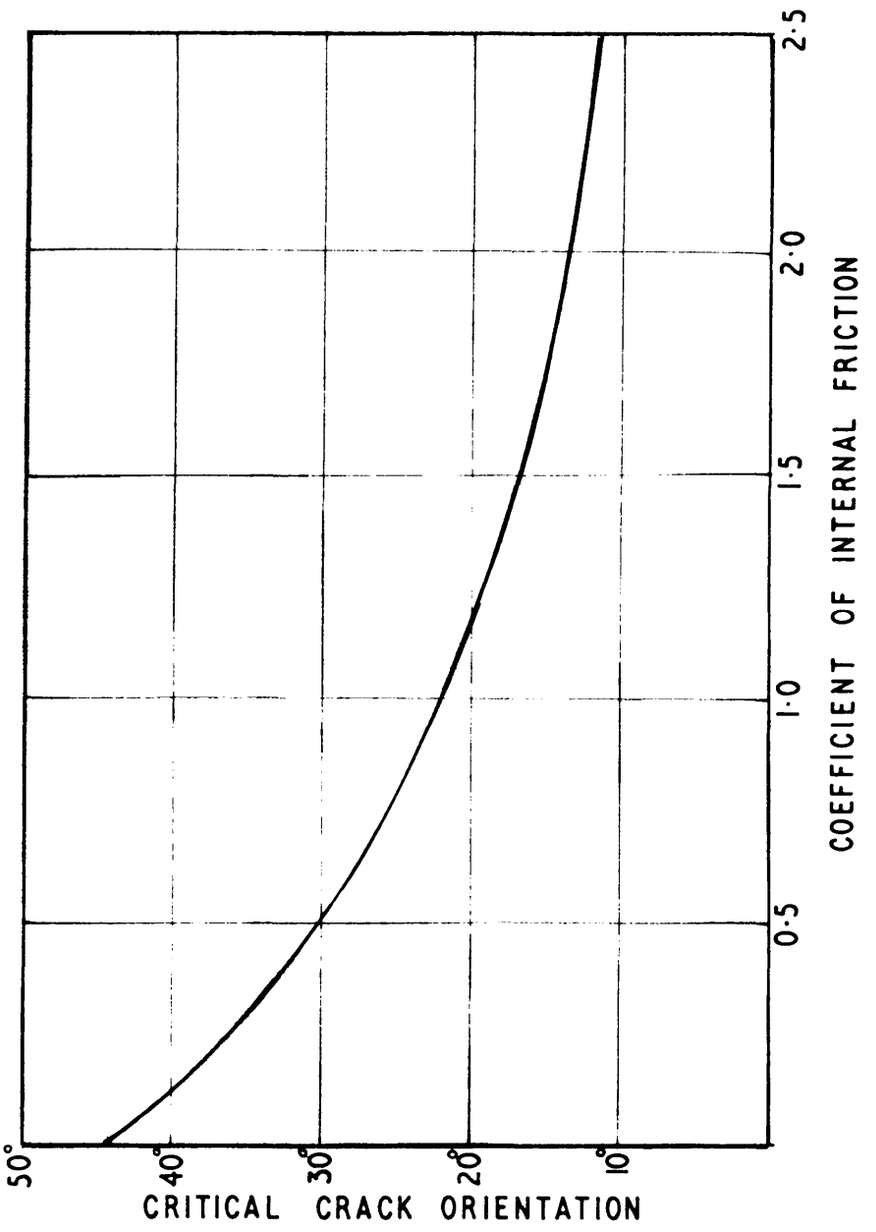

FIGURE 19

ORIENTATION OF THE CRITICAL CRACK FOR VARIOUS COEFFICIENTS OF INTERNAL FRICTION

— AND —

ORIENTATION OF FRACTURES ACCORDING TO ANDERSON (1951)

5.2.5. Influence of size on the strength of materials.

The uniaxial compressive strength as given in Table I were determined on selected specimens. It is known that the rock mass is traversed by numerous cracks and joints and this would have the effect of lowering the strength mentioned above with increase in the size of the specimen.

Weibull (Lundborg, 1967, pp.269-272) developed a formula by which he could calculate the decrease in strength with increase in the size of the specimen. He employs a certain constant which is a function of the number of cracks and joints, and calculated the curve given in Fig. 20 for a value of m = 12. This curve illustrates that the strength of a granite mass is about half of the uniaxial compressive strength determined in the laboratory.

5.2.6. Influence of moisture on the strength of quartzitic shale.

Colback and Wiid (1965, p.65) showed that the moisture content has a major influence on the compressive strength of rock and that, if rock-strength values are presented without reference to moisture content, it is difficult to compare and correlate data from different sources, as well as to know the actual strength of a rock underground. For instance, the uniaxial compressive strength of a specimen of quartzitic shale dried over $CaCl_2$ is 27,000 p.s.i., but in an atmosphere of 98 per cent relative humidity the strength is reduced to 15,000 p.s.i.

The uniaxial compressive strengths given in Table I were obtained from air-dried specimens.

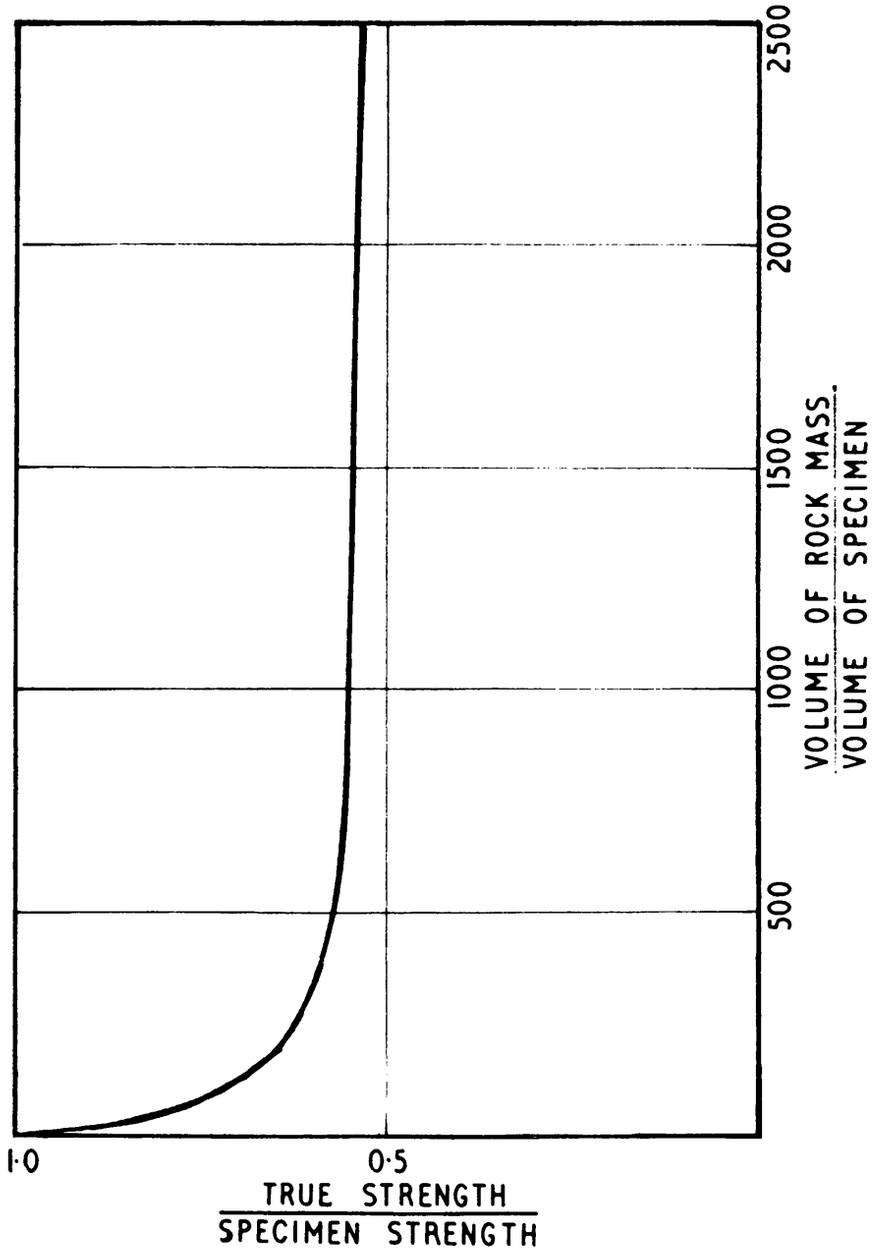

FIGURE 20

INFLUENCE OF THE SIZE OF THE SPECIMEN ON THE STRENGTH OF GRANITE

6. PREDICTION, AND COMPARISON WITH MEASURED VALUES:

The first step is to determine the extent of fracturing in the present environment. For this purpose the following must be known:

(a) The values of the maximum principal stress for various distances ahead of the face, and for different stope spans. This can be read from Fig. 13.

(b) The distribution of the k-ratio given in Fig. 14.

(c) The uniaxial compressive strength of the quartzite.

(d) The coefficient of internal friction.

The uniaxial compressive strengths given in Table I are for selected specimens of quartzite and the influence of size (5.2.2.5) as well as the influence of moisture content (6.2.6.) are completely disregarded. For the present investigation values of 22,000 p.s.i. and 18,000 p.s.i. are used. These two values are the limits within which it is assumed that the rock strength would lie under conditions prevalent in the hanging-wall strata of this stope.

The coefficient of internal friction of argillaceous quartzite is assumed to be 0.5. This value was selected because the difference between mean values of Class I and Class III fractures is 30 degrees. This, according to Fig. 19, will result if a rock has a μ-value of 0.5.

6.1. Distance of fracturing ahead of face.

Figs. 21 to 25 give the extent of fracturing for stope spans between 40 and 200 feet. For a stope span of 0 feet to 120 feet,

σ_1 = MAXIMUM PRINCIPAL STRESS.

σ_3 = MINIMUM PRINCIPAL STRESS.

σ_c = UNIAXIAL COMPRESSIVE STRENGTH

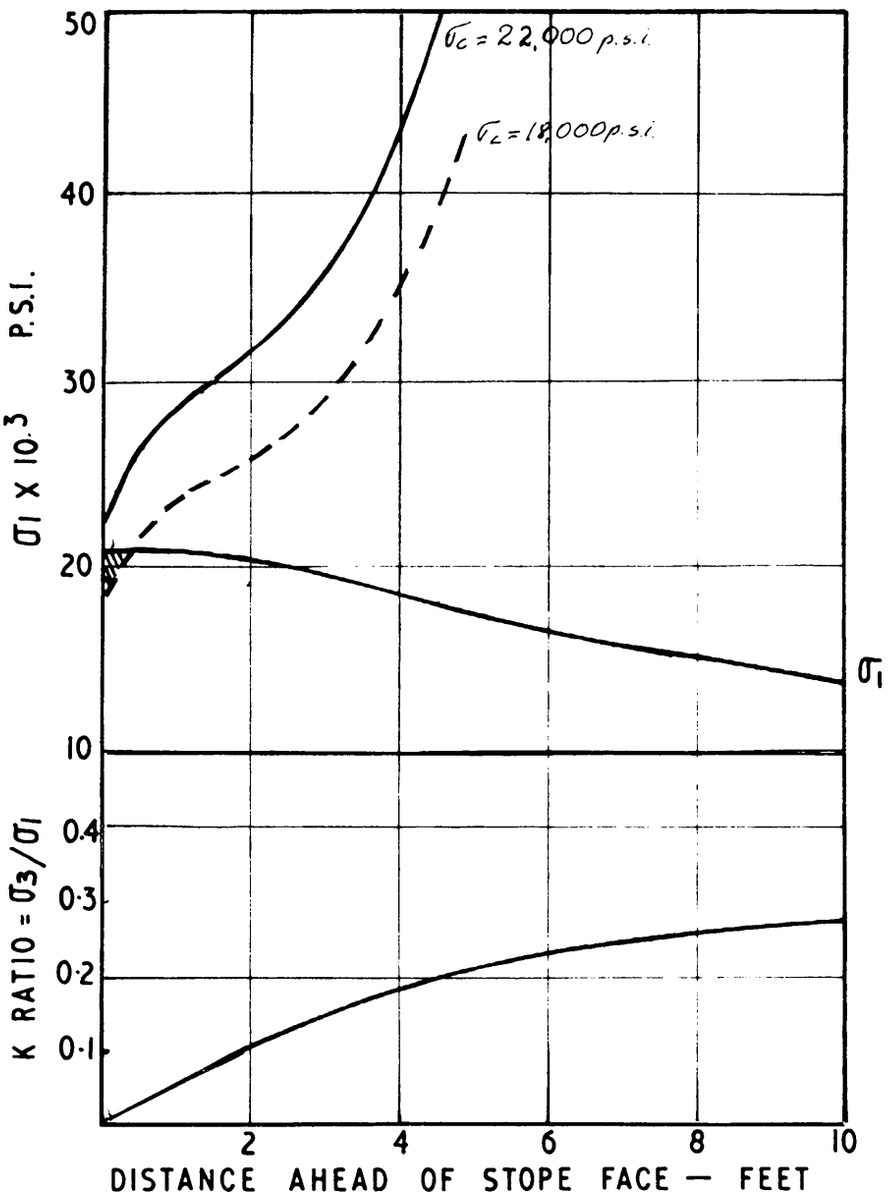

FIGURE 21

EXTENT OF FRACTURE INITIATION AT A STOPE SPAN OF 40 FEET.

σ_1 : MAXIMUM PRINCIPAL STRESS

σ_3 : MINIMUM PRINCIPAL STRESS

σ_c : UNIAXIAL COMPRESSIVE STRENGTH

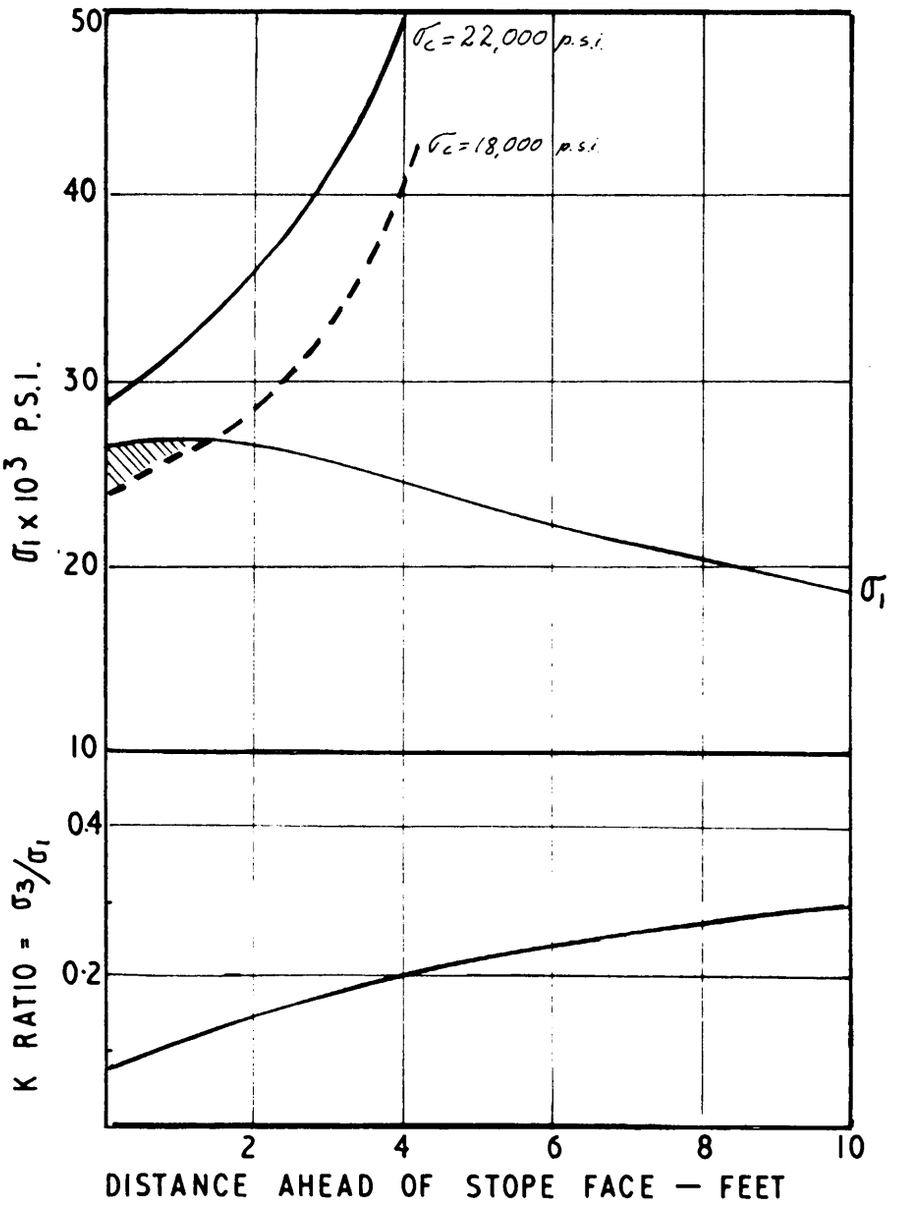

FIGURE 22

EXTENT OF FRACTURE INITIATION AT A STOPE SPAN OF 80 FEET.

σ_1 : MAXIMUM PRINCIPAL STRESS

σ_3 : MINIMUM PRINCIPAL STRESS

σ_c : UNIAXIAL COMPRESSIVE STRENGTH

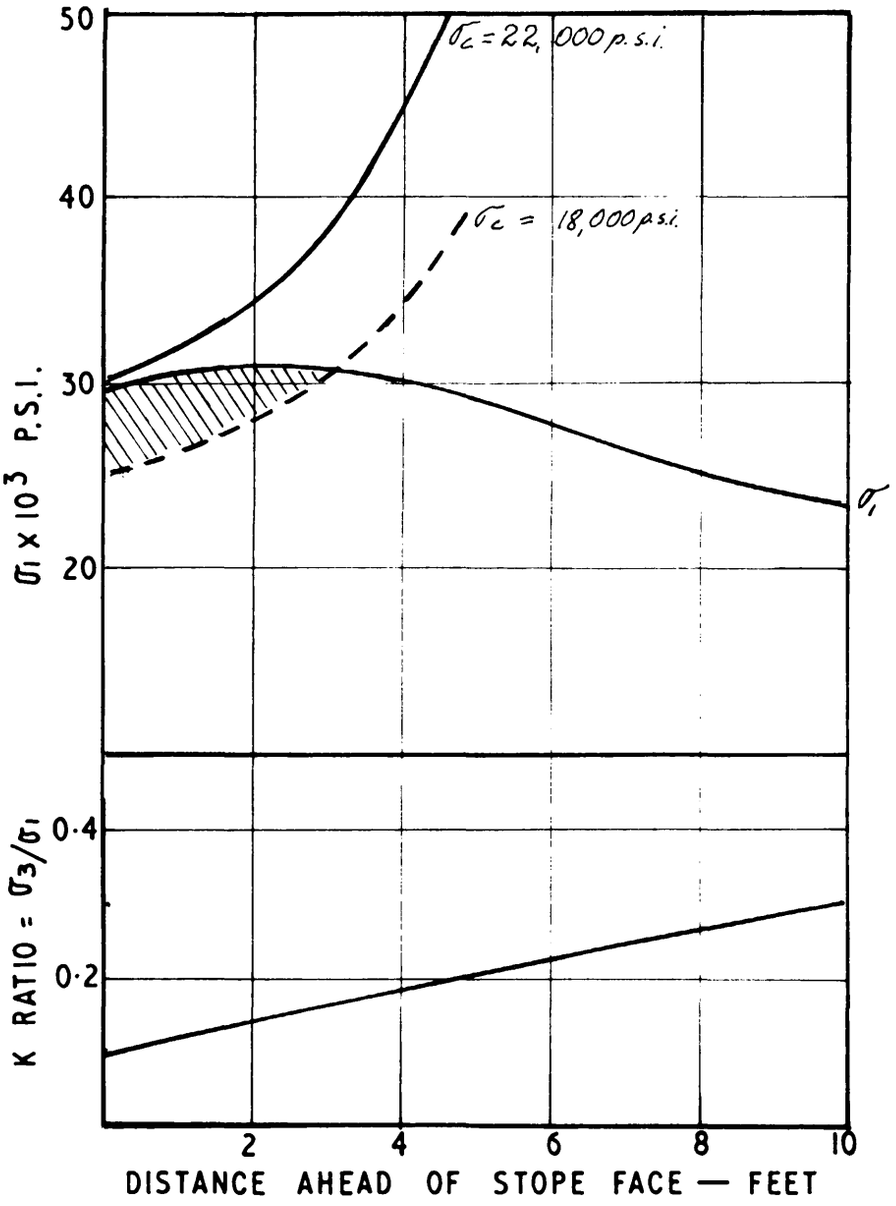

FIGURE 23

EXTENT OF FRACTURE INITIATION AT A STOPE SPAN OF 120 FEET.

σ_1 = MAXIMUM PRINCIPAL STRESS

σ_3 = MINIMUM PRINCIPAL STRESS

σ_c = UNIAXIAL COMPRESSIVE STRENGTH

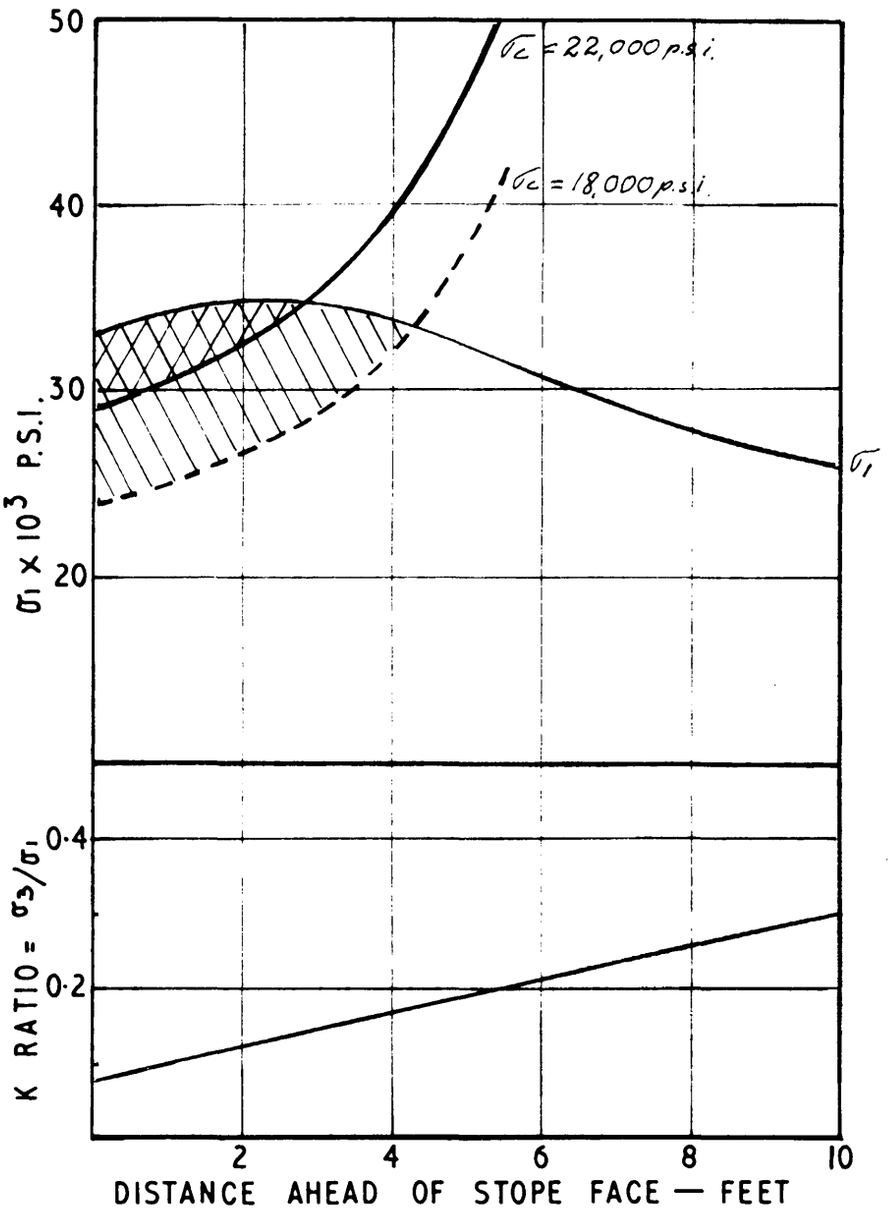

FIGURE 24

EXTENT OF FRACTURE INITIATION AT A STOPE SPAN OF 160 FEET.

σ_1 : MAXIMUM PRINCIPAL STRESS

σ_3 : MINIMUM PRINCIPAL STRESS

σ_c : UNIAXIAL COMPRESSIVE STRENGTH

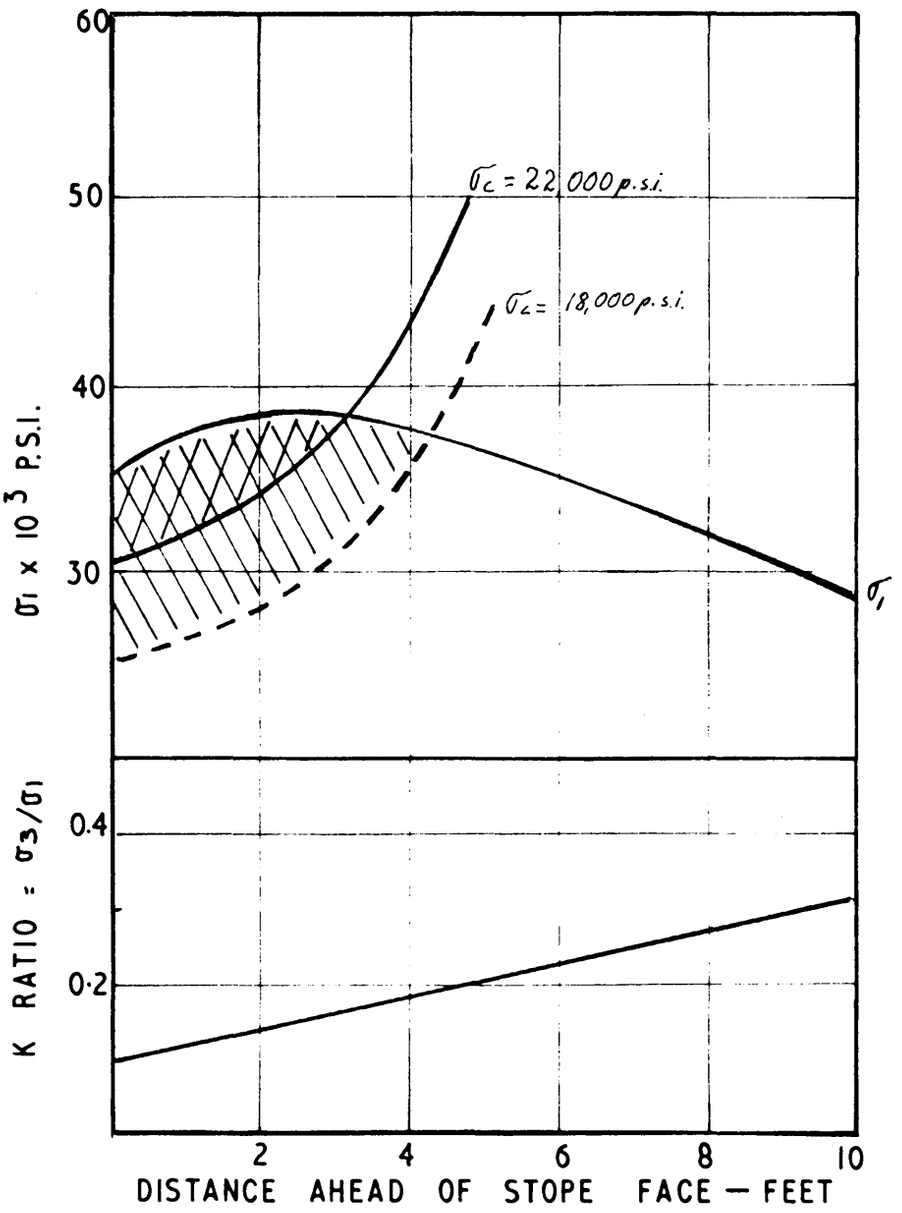

FIGURE 25

EXTENT OF FRACTURE INITIATION AT A STOPE SPAN OF 200 FEET

no fracturing should take place if the uniaxial compressive strength is 22,000 p.s.i. but in the case of a strength value of 18,000 p.s.i., fractures should appear at a span of approximately 30 feet. These distances are summarised in Fig. 26.

Fig. 30 shows that fractures do not occur at spans of less than 120 feet and it must therefore be assumed that the uniaxial compressive strength of the rock is less than 22,000 p.s.i.

In Figs. 21 to 25 it is assumed that fracturing occurs instantaneously and that the stress distribution will remain the same as in the case of the continuous material. This is difficult to envisage, and two limiting conditions can be imposed on the possible change in the stress distribution after initial failure.

(a) If the fractured rock is unable to support any weight, the stress distribution is carried forward and the fracturing should be self-propagating. This was not the case in stope 29 S 11.

(b) Results by Wiebols and collaborators (1968) show that a fractured material can carry appreciable loads if the confining stress is high enough. Therefore, if the k-ratio is not changed after fracturing, the zone should extend as given in Figs. 21 to 25.

The actual case would lie between these two extremes, but the distance of fracturing cannot be compared with measurements, as none was made at the time.

6.2. Orientation of fractures.

The orientation of fractures can be predicted if the

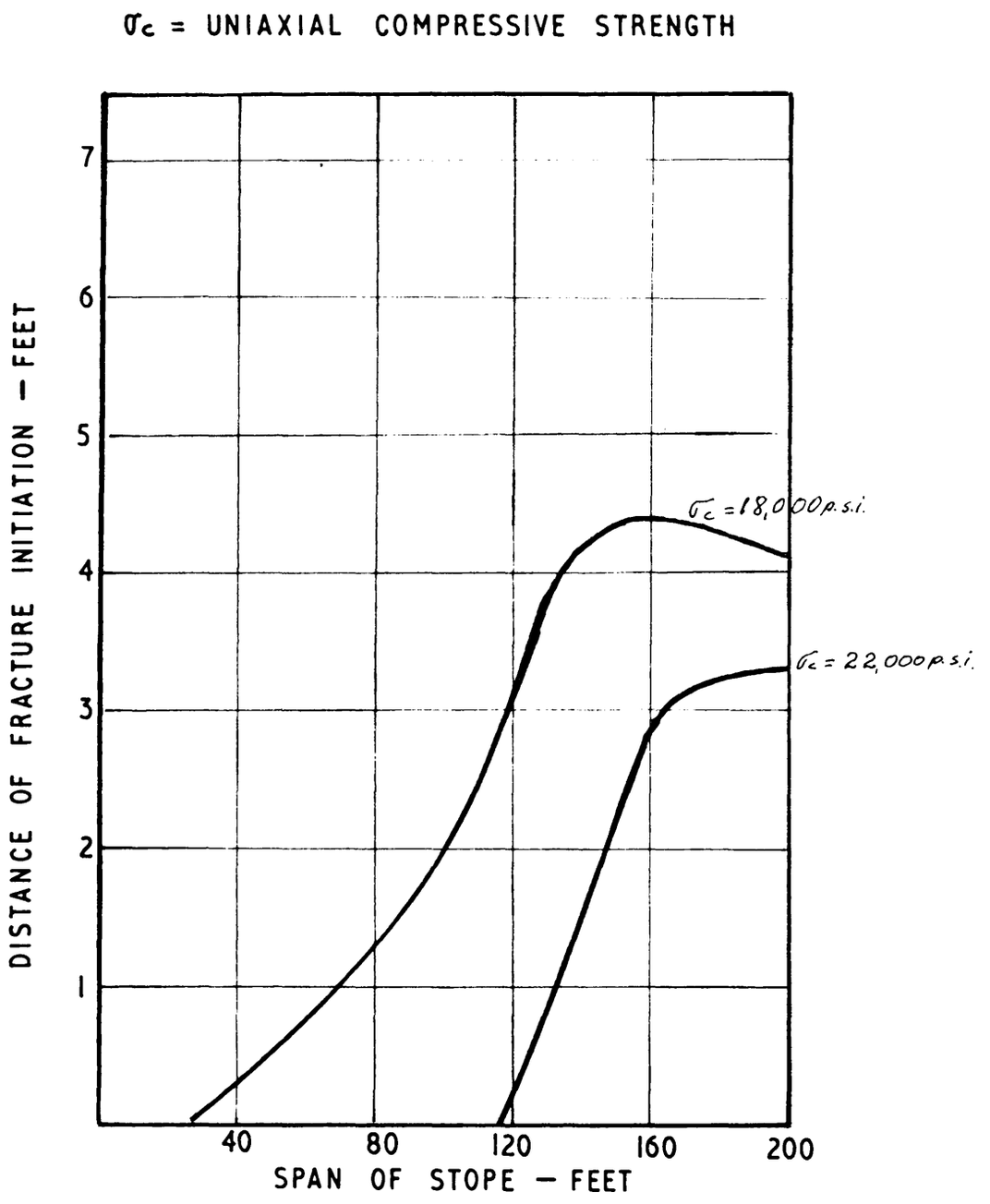

FIGURE 26

EXTENT OF FRACTURE INITIATION FROM AHEAD OF STOPE FACE FOR INCREASE IN STOPE SPAN.

following factors are known :-

(a) The orientation of the maximum principal stress at various distances ahead of the face for various stope spans; this is given in Fig. 15.

(b) The angle of shear of the rock which is 30 degrees for a coefficient of internal friction of 0.5.

(c) The average advance per blast, which in stope 29 S 11 was 3 feet.

Figs. 27 to 29 give the predicted orientation of fractures for stope spans of 120, 160 and 200 feet. On these figures, the orientation of the maximum principal stress is given for a distance of 0 to 5 feet in front of the stope face. The theoretical orientation of the fractures can then be predicted by adding or subtracting 30 degrees from this value. (In Figs. 27 to 29, 30 degrees were added because the majority of measured values (99.9%) lie in the region between 50 and 120 degrees).

Assuming that the face advanced 3 feet per blast, the fracture orientation should follow a "saw-tooth" pattern as shown in Figs. 27 to 29. (This pattern would also be a function of the distance of fracturing as discussed in the previous section).

Superimposed on these graphs are measured values at corresponding stope spans. This poses a problem in that the position of the face for the theoretical distribution is defined clearly, but what was the face position for a specific fracture that had been measured? The reasoning here was to take the lowest value of one cycle as corresponding

with the face position, but it was found that this did not improve the correspondence between the predicted and the measure values substantially. Therefore, the measured values were shifted so as to obtain as close a fit as possible.

For a further discussion Figs. 27 to 29 will be described separately :-

(a) Fig. 27. Theoretically the fractures should lie between 95 and 105 degrees, over a distance of 3 feet for a rock with a uniaxial compressive strength of 18,000 p.s.i. The measured values occasionally fall in this region but are mainly concentrated between the orientation of maximum principal stress and the theoretical fracture orientation. The measured values do exhibit the "saw-tooth" effect but the frequency and amplitude do not correspond with predictions.

There is obviously some discrepancy between the two sets of data, and the reason could be that the assumptions made for the theoretical model are incorrect, or that the fracture criterion is not applicable.

However, the prediction can be used to delimit the orientation between which the fractures will most probably lie.

(b) Fig. 28. A quartzite with a uniaxial compressive strength of 22,000 p.s.i. will fracture for a distance of 3 feet ahead of the face. This corresponds with the advance of the face per blast. The correspondence between predictions and measured values is better than in the case of Fig. 27, but the discrepancy between the amplitude and the frequency is still pronounced.

SPAN OF STOPE = 120 FEET

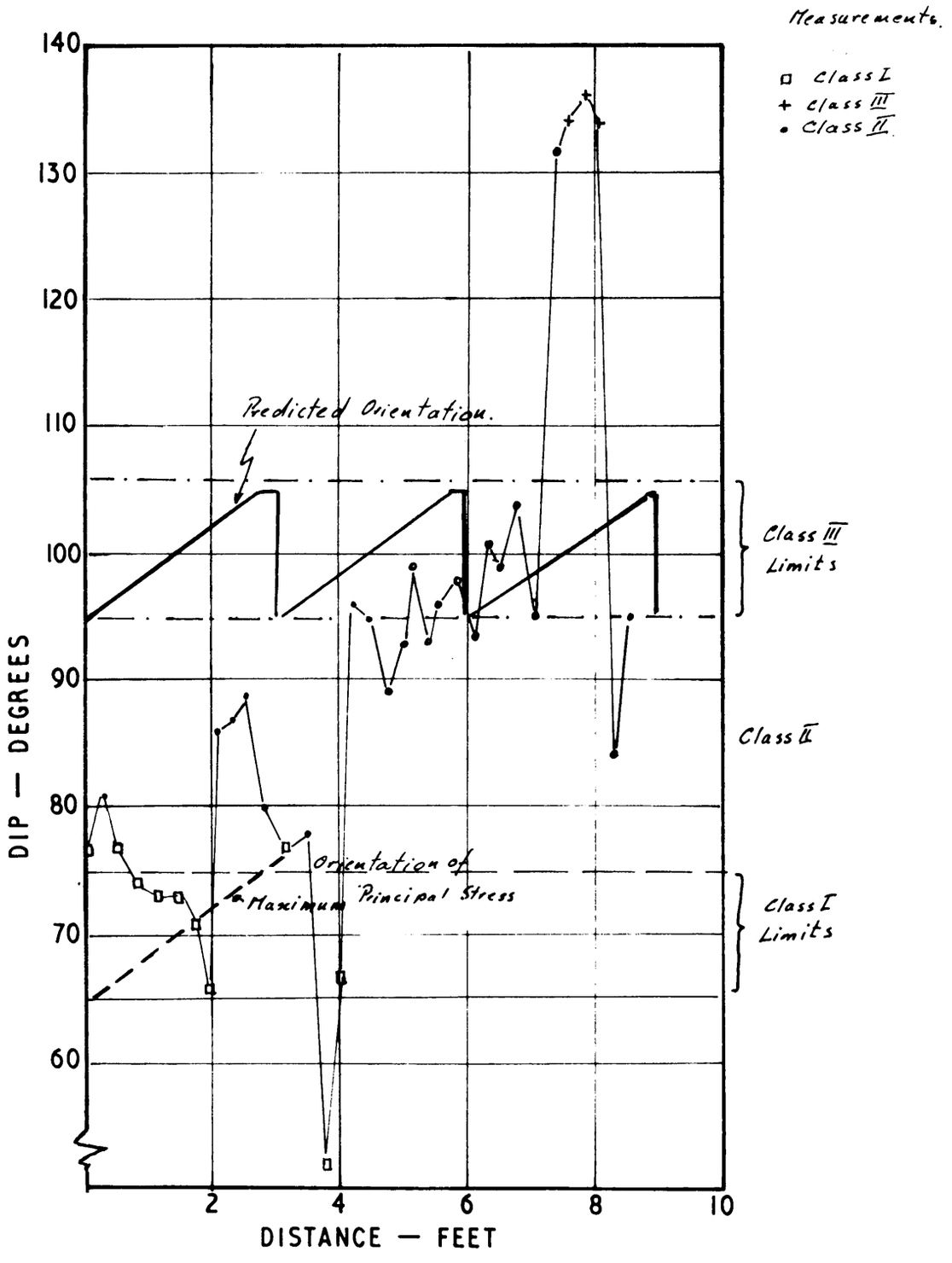

FIGURE 27

COMPARISON BETWEEN MEASURED AND PREDICTED ORIENTATION OF FRACTURES

SPAN OF STOPE 160 FEET

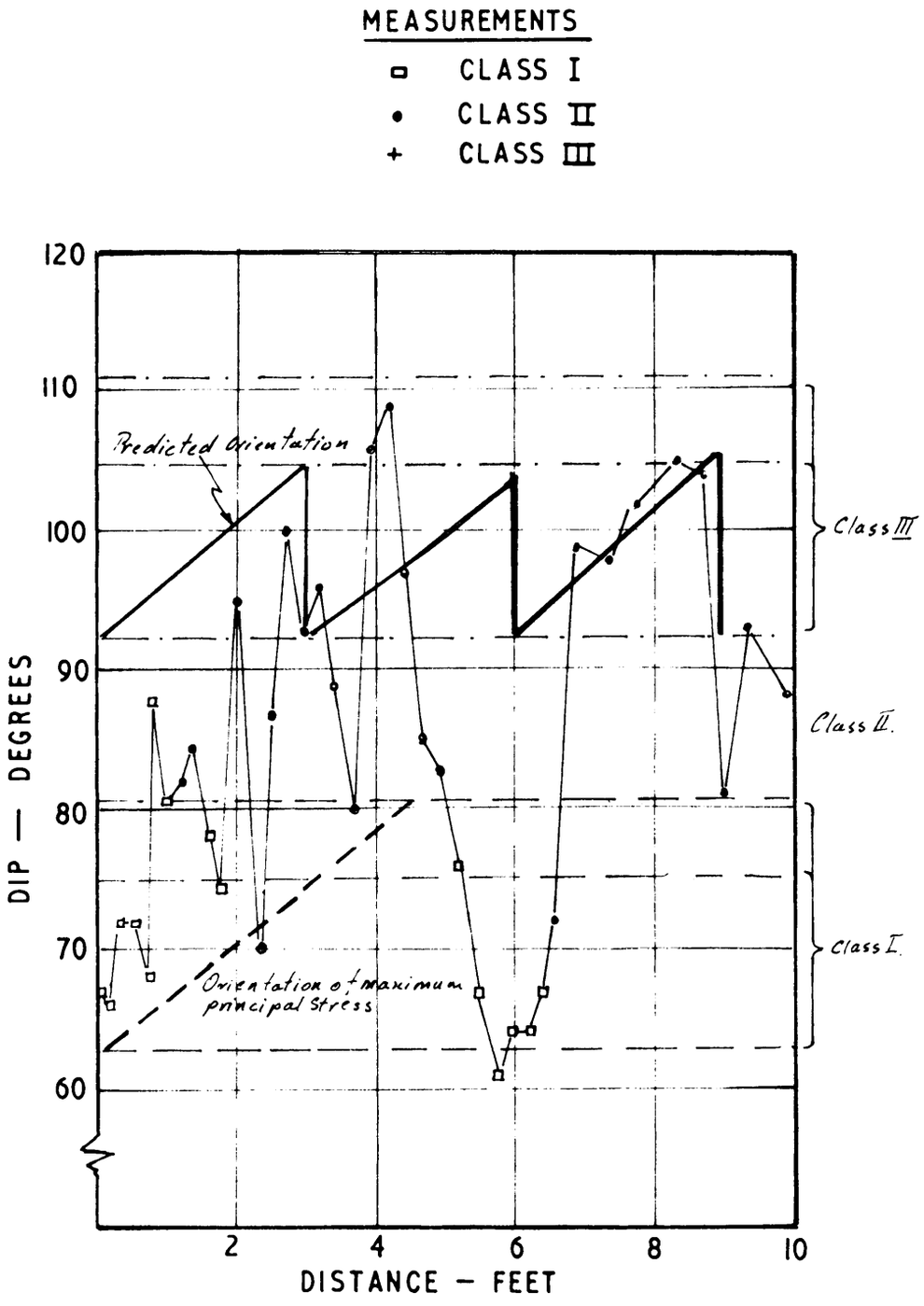

FIGURE 28

COMPARISON BETWEEN MEASURED AND PREDICTED ORIENTATION OF FRACTURES.

If the strength of the quartzite is 18,000 p.s.i. another complication arises. In this instance the theoretical fracture zone extends for 4 feet ahead of the face, this is one foot in excess of the advance in one blast. This implies that before the face is advanced again there already exists a zone of fractured material over a width of one foot. This could result therein that the k-ratio is reduced in this already fractured material and this could be the reason for the eceptionally low values which fall in the region of the orientation of maximum principal stress. Alternatively, the predicted stress distribution is completely changed by the one foot of fractured material, in which case the prediction would be completely inaccurate. From the correspondence between the two sets of data this does not seem to be the case.

From the above discussion it is concluded that either the rock is stronger than 18,000 p.s.i., or that the existing one foot of fracturing does not alter the stress distribution significantly.

(c) Fig. 29. The same arguments are applicable as in Fig. 28. The scatter in the orientation of fractures is less, and they coincide more closely with predicted values. This could be the result of a higher restraint of the already broken rock, which therefore acts more like the solid which has been assumed in the model. This increase in restraint could be the result of a condition where the actual face position is in advance of the apparent face position, i.e. the fractures originate not in the actual face but a few feet in advance of this. This would also explain the reduction in the scatter of the values, as the change in the orientation of the maximum principal stress is less drastic 10 feet in front of the face as in the region between 0 and 4 feet. (Fig. 15).

SPAN OF STOPE 200 FEET

MEASUREMENTS

\+ CLASS III

• CLASS II

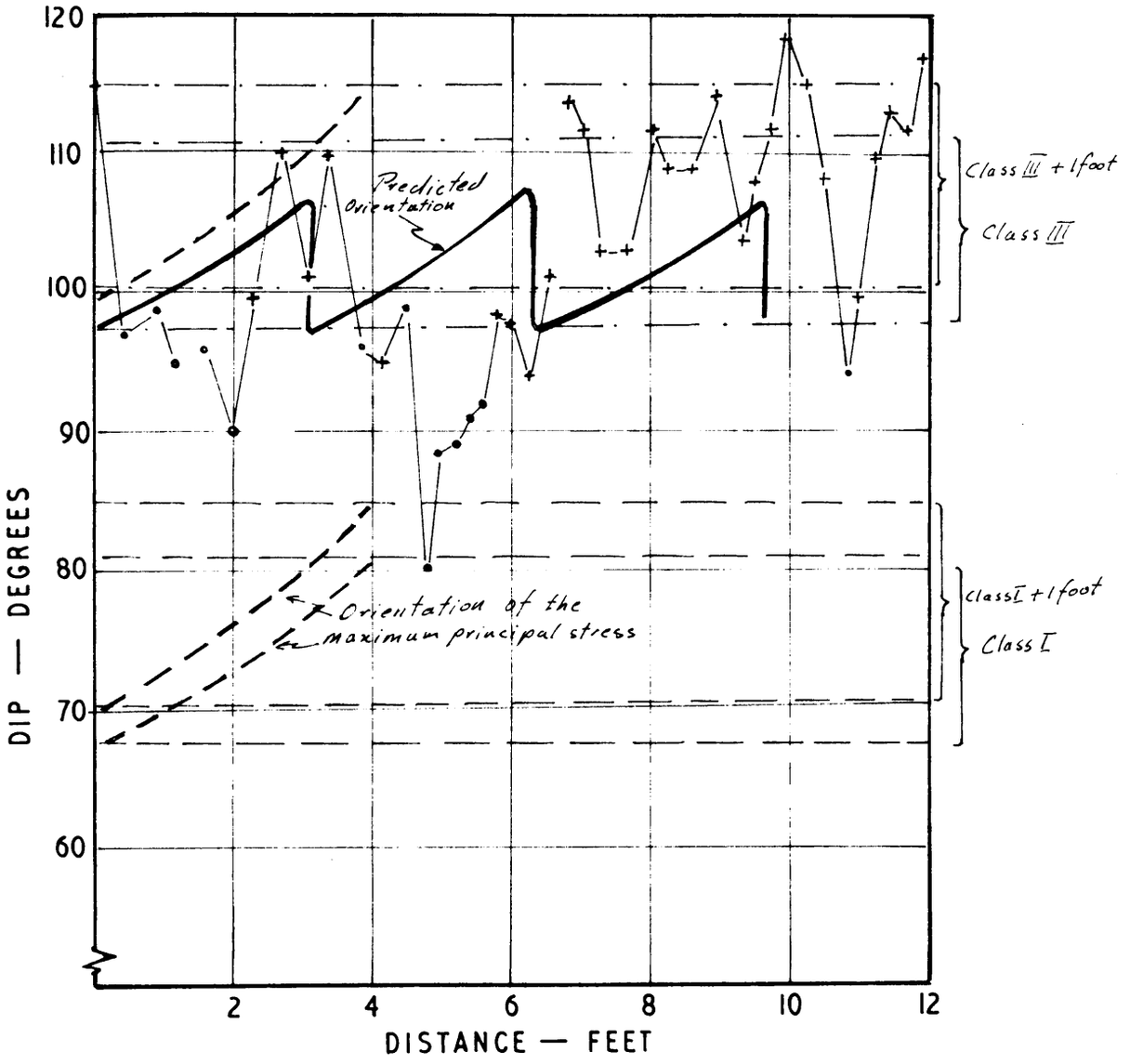

FIGURE 29

COMPARISON BETWEEN MEASURED AND PREDICTED ORIENTATION OF FRACTURES.

For example, if the fractures originate one foot ahead of the face, and the existing stress distribution is not materially changed, the resultant orientation is shown in this figure. This could explain why the measured values fall beyond the limit of orientation of the Class III fracture.

From this comparison it is obvious that the limits within which the fractures lie can be determined, but the actual frequency and amplitude of the curve cannot as yet be simulated.

6.3. Frequency of fractures.

Fig. 30 is a plot of the average frequencies of fractures in the first and second layers in the hanging wall, in the first and second panel of stope 29 S 11. The curves show that there is a reduction in frequency with increase in stope span.

Price (1959, p.162) believes that the joint frequency is related to the strain energy stored in the rock. The strain energy in an elastic material is half of the product of the stress times the resultant strain. This means that the strain energy before fracturing must increase with increase in stope span. However, the frequency decreases, therefore, the above assumption is incorrect, or some other mechanism is involved.

In Figs. 5 and 6 there is an apparent increase in the recognised Class III fractures in terms of the stope span. It appears that Class I fractures decrease whereas Class III fractures increase in relative frequency. This could mean that the increase in stored strain energy with increase in span is dissipated to a greater extent in Class III fractures than in the case of Class I fractures. Class III fractures exhibit definite signs of movement compared with Class I fractures where no such signs exist. This movement must have the effect of reducing available energy more than

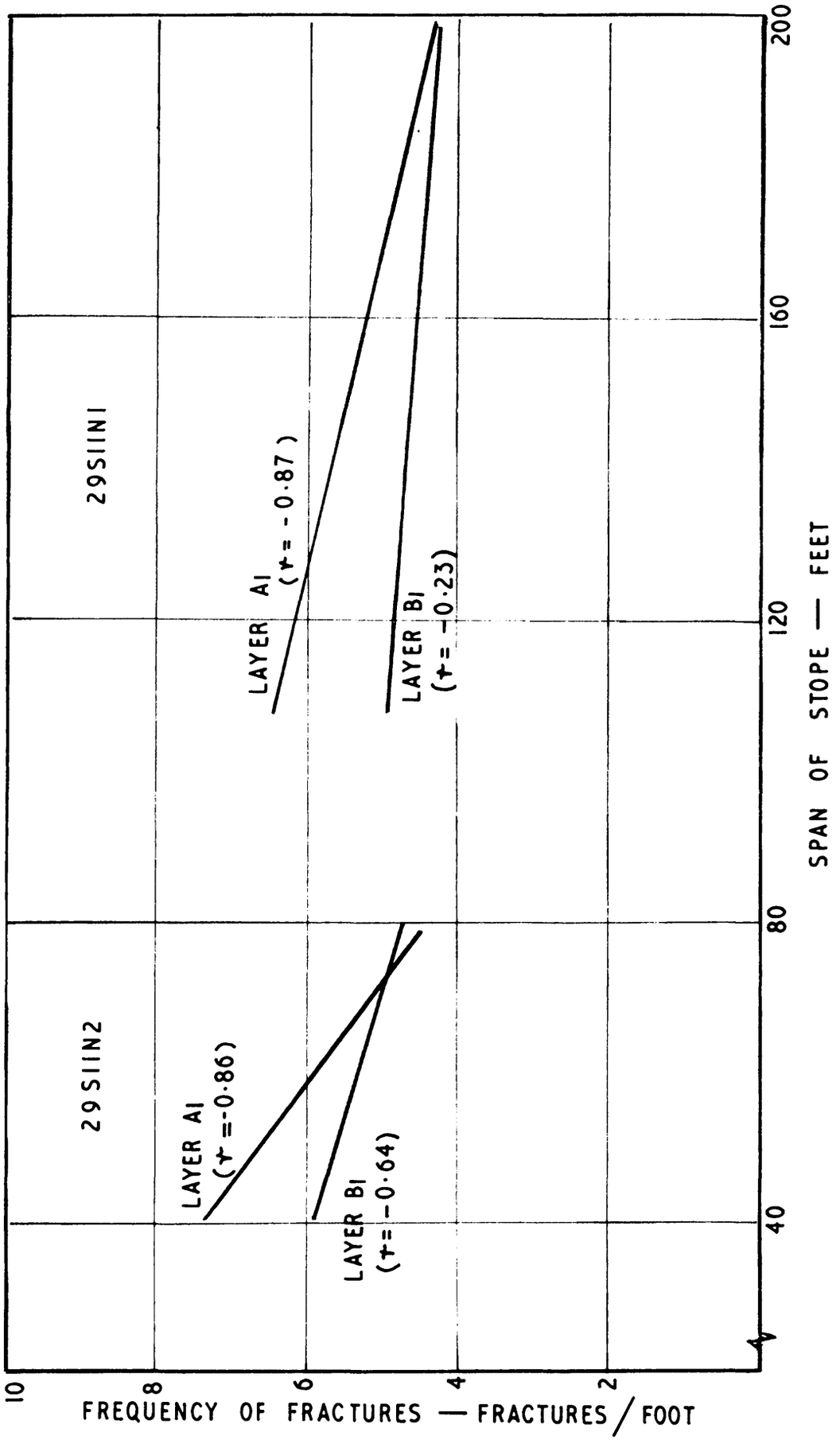

FIGURE 30

LINES OF REGRESSION OF FREQUENCY OF FRACTURES FOR DIFFERENT SPANS OF A STOPE.

in the case of supplying surface energy only necessary in the case of fractures of Class I.

6.4. Influence of layering.

In the course of this discussion the layering, or inhomogeneity, of the hanging wall of Stope 29 S 11 has been completely disregarded. Fig. 9 shows that the argillaceous layers have an influence on the orientation of fractures. However, where the argillaceous layer becomes less than 2 inches in thickness, this influence is not obvious and the fracture orientations used for the previous discussion were measured across where the argillaceous plane was less than 2 inches in thickness, or absent.

The influence of the bedding plane could give rise to the anomaly between measured and predicted values. However, this cannot be tested at present and although very important from a tectonic point of view, must be left in abeyance for the time being.

6.5. Classification of fractures.

Figs. 27, 28 and 29 also show the various classes of fractures which have been recognised underground. According to the failure criterion all the fractures should exhibit features of Class III fractures. From the plotted data it is obvious that this is not the case, as Class I and Class II fractures predominate in Figs. 27 and 28.

Class II fractures coincide with the predicted fracture orientation, while Class I fractures approximately follow the orientation of the maximum principal stress (Fig. 27). Three Class III fractures appear 30 degrees above the average predicted values.

In Fig. 28 fractures of, once again, Class I tend to lie in the region of the orientation of the maximum principal stress, but fractures of Class II cover the area between Class I and fractures predicted. No fractures of Class III appear.

At a stope span of 200 feet (Fig. 29) fractures of Class III predominate and fall within the regions of the predicted orientation of fractures. Occasional fractures of Class II appear between predicted fractures and the orientation of the maximum principal stress.

6.6. Discussion.

The orientation of fractures can be predicted to a certain degree of accuracy. The correspondence at this stage is that the limits of the orientations can be predicted in the present environment, as well as the general change in orientation, i.e. the "saw-tooth" pattern.

However, the individual values may differ from predictions by as much as 40 degrees and the reason for this can be the result of a number of factors. It will be useful here to recall all the assumptions again to see whether anything could be changed to give a closer fit.

6.6.1. The stress distribution.

The basic assumptions in the calculation of the stress distribution was that of a flat ellipse lying in a homogeneous, isotropic and elastic medium. From the detailed geological column (Table II) it is clear that the material is not homogeneous over a distance of 3 feet in the hanging wall. Measurements made by the C.S.I.R. (1963) showed that the argillaceous quartzite has time-dependent properties and, therefore, deviates from linear elasticity. The influence of these two (inelasticity and inhomogeneity) factors cannot be assessed at present by available

techniques. The finite element method (Anderson and Dodd, 1966, p.317) can be used to simulate the influence of layering, but the time-dependent properties cannot be incorporated at present, but as computer capacity increases, this problem can be solved.

Another important factor in the stress distribution could be the change in the method of support. A close inspection of Figs. 5 and 6 shows a definite change in the trend of the orientation of fractures as soon as caving commenced. This could result therein that, as soon as the hanging wall has broken behind the last row of hydraulic props, lateral movement into the stope takes place. This movement has been measured (approximately one inch relative movement between hanging wall and foot wall). The effect of this lateral movement would be to introduce a couple, and in this manner steepen the orientation of the maximum principal stress, and could be the reason for the creation of fractures in Class III with values in excess of those predicted. (See Fig. 27).

From this discussion it is clear that the knowledge of the absolute distribution of stress is subject to a number of influencing factors of unknown magnitude.

6.6.2. Failure criterion.

The modified Griffith failure criterion as described by Hoek (1965) has been used for the evaluation of the stress distribution. In the meantime this criterion has been criticised on a number of points.

Hoek and Bieniawski (1965) state that this criterion does not adequately explain the direction and the rate of propagation of fractures under compression and that it is limited to predict conditions of fracture initiation. However, Bieniawski (1967, p.10) concludes that the modified

Griffith criterion can be used as a "phenomenological" strength failure criterion, but it does not constitute, in the form discussed, an hypothesis for a mechanism of propagation of brittle fractures. The main argument here is that the coefficient of internal friction used by Hoek (1965) is not a true coefficient, but an apparent one, and Bieniawski (1967, p.10) maintains that if this apparent coefficient is used, the modified Griffith criterion may be used for strength failure prediction.

Jaeger (1967, p.24) states that under uniaxial compression, and at very low confining pressures (low) splitting of the rock in planes parallel to the direction of greatest compression takes place. This statement is substantiated by observations made by Fayed (1968, p.84) who found that there is a discrepancy between the measured angle of shear and the angle predicted by using Mohr's envelope for k-ratios less than 0.1. From the above it is clear that the critical crack orientation given in Fig. 18 is not necessarily the orientation of the ultimate fracture planes for a k-ratio below 0.1. In a region between 0.1 and uniaxial compression, the orientation of the fracture lies somewhere between being parallel to the direction the maximum principal stress, and the predicted angle of shear.

This means that where the k-ratio is less than 0.1 the prediction of the orientation of fractures becomes difficult as only the limits can be given. In Figs. 23 to 25 the k-ratio has a value of 0.1 and more. If for instance this value decreases, maybe on account of fracturing, vast changes in the orientation can result. This could explain the sudden changes in the orientation of the fractures.

6.6.3. Summary.

It is clear from the above discussion that the influence of -

(a) Inhomogeneity, inelasticity,

(b) failed material,

(c) lateral movement, and

(d) inadequate knowledge about the failure mechanism,

could give rise to discrepancies observed in the comparison of the measured and the predicted orientation as well as the class of fractures.

The influence of the various variables can only be determined by keeping some of them constant. By such a process of elimination it would be possible to determine their influence. This will be an investigation on its own and the writer is at present proceeding therewith.

7. CONCLUSION, WITH SPECIAL REFERENCE TO TECTONIC ANALYSIS:

The purpose of this investigation was to make a controlled macroscale experiment of the failure of rocks subjected to a known load. From the results obtained it is clear that a number of variables make it difficult to draw any specific conclusions as to the validity of either the method of calculating the stress distribution around a stope-like excavation, or the validity of the modified Griffith fracture criterion.

However, from a comparison between the measurement and the predicted values it has become clear that the limits within which fractures can be expected to occur can be delineated.

Secondly, the modified Griffith fracture criterion has an advantage over the maximum shear-stress theory, in that it explains the appearance of Class I or so-called tension-fractures. If the maximum

shear stress theory had been used for the predictions, the presence of Class I fractures could not be explained.

Another important point is that the data as measured in the field should first be analysed in the manner discussed here and then only can average values be used. For instance, if an average value of the orientation of fractures were taken over distances of 10 feet, the "saw-tooth" pattern would be obliterated and even fewer conclusions could be drawn.

In addition, Roering (1967) has analysed fractures on a mesoscopic scale and has come to the conclusion that the mechanism governing fracturing on this scale is the same as fracturing on microscopic scale and faulting on the macroscopic scale. This approach is used in this thesis. The knowledge gained from the investigation of fractures around underground excavations can be used to elucidate faulting phenomena on the macroscopic scale. This approach is illustrated by using data published by Olivier (1965, 99. 143-175).

Olivier used underground observations and bore-hole information to determine the structure of the northernmost area of the Orange Free State Gold-field where the various post-Witwatersrand faults and their age relationships show that there were three periods of major tectonic disturbance, viz:

(a) a post-Lower, pre-Middle Ventersdorp period,

(b) a post-Middle, pre-Upper Ventersdorp period, and

(c) a post-Ventersdorp period.

The orientations of the maximum and intermediate principal stresses, and the angle of shear as listed in Table 3 were obtained from the published stereographic projections. These data are used for further analysis.

The angles of shear listed in Table III can be used to determine the coefficient of internal friction (μ). If μ approaches zero the material tends to behave like a plastic material, and if μ is in excess of 1.0 the behaviour of the rock is essentially brittle. Therefore the coefficient of internal friction is useful to determine the physical condition in which a material was when a conjugate fracture system originated. (This physical condition naturally is a function of the grade of consolidation, temperature, pressure and amount of water present. Therefore a value of μ can be used to speculate on these various aspects).

Angle of Shear. The coefficient of internal friction, determined from the angle of shear (Fig. 19) can give some information about the physical properties of the material or the stress ratios during any specific period. In Table 3 the coefficients of internal friction are given for the different major tectonic periods.

(a) Relatively low values of μ , of 0.49, 0.14 and 0.21, for the Middle Witwatersrand period means that the material was still in an unconsolidated state, or that the compressive forces were such that the quartzites (sandstone ?) reacted in a plastic manner. Olivier (1965 p 193) concluded that there is a relationship between sedimentation and contemporaneous folding and overthrusting, which implies that the material was not fully consolidated.

TABLE 3

TECTONIC HISTORY OF LORAINE GOLD MINE AREA

WITWATERSRAND AGE		VENTERSDORP AGE			POST-VENTERSDORP AGE
		Lower pre-Middle Ventersdorp Age		Post Middle pre-Upper Ventersdorp Age	
		Pre-Westerly Tilt	Westerly Tilt		
Faults	Thrust faults 10, 19 and 21	VDH6 & TV2	Uitkyk and No. 4 Fault	Weltevrede and TV3 Fault	Freddies fault and Fault C
				Rosedale Fault	Statistical results
σ_1	N 105 W	N 2 E	Vertical	Vertical, Vertical	N 85 E, N 98 E
σ_2	N 15 W, N 12 W	N 88 W	N 10 W	N 55 E, N 40 E	Vertical, Vertical
α	32°, 41°, 39°	44°	21°	15°	30°, 28°
μ	0.49, 0.14, 0.21	0.04	1.11	1.74	0.58, 0.68
Period		2	3	(4 + 5)	6

Where σ_1 = Maximum principal stress orientation

σ_2 = Intermediate principal stress orientation

α = Angle of shear

μ = Coefficient of internal friction

(b) A value for the coefficient of friction of 0.04 for the pre-Middle Ventersdorp age means that :-

(i) the material was not completely consolidated, i.e. in a high plastic state, or

(ii) the stress field was nearly hydrostatic, and as a result the material behaved in a more plastic manner, or

(iii) the orientation of the maximum principal stress was not the same in the vicinity of bore-holes TV2 and VDH6 respectively.

Since the value of the coefficient of friction was in excess of 0.04 in the preceding (Middle Witwatersrand) period, it is thought unlikely that the material became more plastic with time. In this case the assumption of near hydrostatic stress conditions with an increased plastic response was likely to have been active. This could be the beginning of the change in the orientation of the maximum principal stress to vertical in period 3.

(c) During period 3 a coefficient of internal friction of 1.11 is deduced. This corresponds with values obtained in specimens of chert and very brittle quartzites. This would mean that the quartzites were in a fully consolidated state, as they are now, or that the k-ratio had a value less than 0.1.

(d) During periods 4 and 5, post-Middle, pre-Upper Ventersdorp age, the value of μ increased to 1.74. No known rock exists with such a high coefficient of internal friction. It is assumed that the k-ratio was below 0.10 and, therefore, the angle of shear cannot

be determined from this coefficient. This would imply a change from near hydrostatic conditions in period 2, to a condition where the lateral confining pressures were very low, i.e. in periods 4 and 5.

(e) A sudden change between period 5 and 6 resulted in a horizontal maximum principal stress with change in the value of μ as determined from conjugate faults. 0.58 and 0.68 are within the region of values measured on specimens of some argillaceous quartzites. Since the rocks in this area are mainly highly siliceous, of which one would expect μ values close to 1.0, it is thought that the vertical compressive stress did not reduce significantly but that the horizontally orientated intermediate principal stress increased substantially. This would result in a stress field approaching hydrostatic conditions and it is considered that the quartzites reacted in a more plastic manner, i.e. a reduction of the coefficient of internal friction. This could also be a result of an increase in temperature; the effect would be a reduction in μ.

The orientation of the principal stresses remained nearly constant for all the periods, permitting the summary below :-

Orientation \ Period	1	2	3	4	5	6
Vertical	σ_3	σ_3	σ_1	σ_1	σ_1	σ_2
N20W	σ_2	σ_1	σ_2	σ_3	σ_3	σ_3
N70 E	σ_1	σ_2	σ_3	σ_2	σ_2	σ_1

The maximum principal stress changed from horizontal to vertical gradually, then suddenly, during period 6 reverted to horizontal again.

The orientations as given in the above summary, are similar to those deduced by Olivier. In addition, however, some conclusions with regard to the stress environment, and the nature of the material can be made.

The entire sequence of events can be reconstructed in firstly, a period of unconsolidated material subjected to a horizontal stress field. As the depth of deposition increased, so did the vertically orientated stress increase, while the horizontal stress still remained relatively high. This resulted in a near-hydrostatic stress field (period 2). With passage of time, the horizontal stress reduced, and as a result of increase in the overburden, the maximum principal stress became vertical (periods 3, 4 and 5). During period 6 a change in the stress field occurred with a resultant high compressive action in all directions, and the maximum principal stress horizontal again, but with an orientation differing from that appertaining to period 1.

(In the above it is assumed that the orientation of the maximum principal stress was constant for a set of conjugate faults).

With the approach given above certain additional limitations can be placed on the physical environment under which the various fault systems developed.

8. ACKNOWLEDGEMENTS:

The author wishes to thank Anglo-Transvaal Consolidated Investment Company, Limited, and the Chamber of Mines of South Africa for permission to submit this paper as a thesis for the degree of Master of Science. Thanks are also due to Dr. M.G. Hearn, Consulting Geologist of this Company, for encouragement and for the provision of facilities for research, and to his typing and draughting staff for assistance in the preparation of the work. Further, the author would express his thanks to the numerous geologists and mining engineers, who, in discussion, have contributed to the author's knowledge.

REFERENCES

ANDERSON, E.M. (1951) "The dynamics of faulting and dyke formation with applications to Britain." 2d Ed.

Oliver and Boyd, Edinburgh.

ANDERSON, H.W. and DODD, J.S. (1966) Finite element method applied to rock mechanics.

Proc. 1st Cong. Int. Rock Mech. Lisbon, 1966, pp. 317-321.

BECKER, G.F. (1893) Finite homogeneous strain, flow and rupture of rocks.

Bull. geol. Soc. Amer., 4, pp. 13-90

BIENIAWSKI, Z.T. (1967a) Mechanism of brittle fracture of rock.

C.S.I.R. Rep. Meg. 580.

BIENIAWSKI, Z.T. (1967b) Mechanism of brittle fracture of rock Part III - Fracture in tension and under long term loading.

Int. Jour. Rock Mech. Min. Sci., 4, pp. 425-430.

BONNECHERE, F. and FAIRHURST, C. (1968) Determination of the regional stress field from "Doorstopper" measurements.

J. S. Afr. Inst. Min. Metal., pp. 520-544.

BRACE, W.F. (1960) An extension of the Griffith theory of fracture to rocks.

J. geophys. Res., 65, No. 10, pp.3477-3480.

BRACE, W.F. and BYERLEE, J.D. (1966) Recent experimental studies of brittle fracture of rock.

8th Symp. Rock Mech. Minnesota, pp.58-81.

BUCHER, W.H. (1920) The mechanical interpretation of joints.

J. Geol., 28, pp. 707-730.

BUCHER, W.H. (1921) The mechanical interpretation of joints.

J. Geol., 29, pp. 1-28.

COOK, N.G.W., HOEK, E. and SALAMON, M.D.G. (1966) Rock Mechanics applied to the study of rock bursts.

J. S. Afr. Inst. Min. Metal., 66, No. 10, pp. 435-528.

COLBACK, P.S.B. and WIID, B.L. (1965)
The influence of moisture content on the compressive strength of rock.
Rep. from 3rd Canadian Symp. Rock Mech.

C.S.I.R. (1963)
Report on the non-elastic properties of rock from borehole 3034 from Hartebeestfontein Gold Mine.
C.S.I.R. Contract report C,Meg/563.

FAYED, L.A. (1968)
Shear strength of some argillaceous rocks.
Int. J. Rock Mech., 5, No. 1, pp. 79-85.

GRIFFITH, A.A. (1921)
The phenomena of rupture and flow in solids.
Royal Soc. (London) Philos. Trans., 221A, pp. 163-198.

GRIGGS, D.T. (1935)
The strain ellipsoid as a theory of rupture.
Amer. J. Sci., 5th Ser., 30, pp. 121-137.

HAFNER, W. (1951)
Stress distribution and faulting.
Bull. geol. Soc. Amer., 62, pp. 374-375.

HOEK, E. (1965)
Rock fracture under static stress condition.
C.S.I.R. Report Meg 383.

HOEK, E. and BIENIAWSKI, Z.T. (1965)
Brittle fracture propagation in rock under compression.
J. Fracture Mech., 1, No. 3, pp. 137-155.

JAEGER, J.C. (1960)
Shear failure of anisotropic rocks.
Geol. Mag., 97, pp. 65-72.

JAEGER, J.C. (1964)
"Elasticity, fracture and flow with engineering and geological applications."
(Meth. Monographs), John Wiley & Sons, New York.

JAEGER, J.C. (1966)
Brittle fracture of rocks.
Proc. 8th Symp. Rock Mech. Univ. Minnesota, pp. 3-57.

LEITH, A. (1937) — The strain ellipsoid. Amer. J. Sci., 33, pp. 360-368.

LEITH, C.K. (1905) — Rock cleavage. U.S. Geol. Survey Bull., 239.

LUNDBORD, N. (1967) — The strength-size relations of granite. Int. J. Rock Mech. Min. Sci., 4, No. 3, pp. 269-272.

NADAI, A. (1950) — "Theory of flow and fracture of solids." Vol. 1. Engineering Societies Monographs, McGraw Hill Book Co., New York and London.

OLIVIER, H.J. (1965) — The tectonics of the Upper Division of the Witwatersrand System in the Loraine area of the Orange Free State Gold-field. Trans. geol. Soc. of S. Afr., LXVIII, pp. 143-175.

PATERSON, M.S. and WEISS, L.E. (1961) — Symmetry concepts in the structural analysis of deformed rocks. Bull. geol. Soc. Amer., 72, p.872.

PINCUS, H.J. (1951) — Statistical methods applied to the study of rock fractures. Bull. geol. Soc. Amer., 62, pp. 92-93.

PRICE, N.J. (1959) — Mechanics of jointing of rocks. Geol. Mag., 96, pp. 147-167.

RYDER, J.A. and OFFICER, N.C. (1964) — An elastic analysis of strata movements observed in the vicinity of inclined excavations. J. S. Afr. Inst. Min. Met., 64, No. 6.

ROERING, C. (1967) — The geometrical significance of natural en-echelon crack arrays. Univ. Witwatersrand Econ. Geol. Res. Unit, Inf. Circ., 34, pp. 1-11.

ROSS, J.V. (1967) Techniques in structural analysis. Recent advances in Earth Sci.

1966-1967 Session, Exterior Dept., Univ. Brit. Columbia.

SALAMON, M.S.D. (1963) Elastic analysis of displacements and stresses induced by mining of seam or reef deposits.

J. S. Afr. Inst. Min. Metal., 64, No. 4.

SAVIN, S.M. (1961) "Stress concentrations around holes".

Pergamon Press.

TIMOSHENKO, S. and GOODIER, J.N. (1959) "Theory of Elasticity", 2d Ed.

McGraw Hill Book Co., New York and London.

TURNER, F.J., and WEISS, L.E. (1963) "Structural analysis of metamorphic tectonites". Int. Ser. on the Earth Sci.

McGraw Hill Book Co., New York and London.

WAGER, L.R. (1931) Jointing in the Great Scar limestone of Craven and its relation to the tectonics of the area.

Quart. J. geol. Soc. Lond., 87, pp. 392-424.

WEGMANN, C.E. (1963) Tectonic patterns at different levels. A.L. du Toit Memorial lectures No. 8,

Trans. geol. Soc. S. Afr., LXVI, Annexure.

WIEBOLS, G.A. and COOK, N.G.W. (1968) An energy criterion for the strength of rock in polyaxial compression.

Int. J. Rock Mech. & Min. Sci., 5, No. 6

WIEBOLS, G.A., JAEGER, J.C. and COOK, N.G.W. (1968) Rock property tests in a stiff testing machine.

Unpubl. Report, Mines Research Lab. Chamber of Mines of S. Afr.

WILSON, N.L., OOSTHUIZEN, D.H. BRINK, W.C.J., TOENS, P.D. (1964) The geology of the Vaal Reef Basin in the Klerksdorp area, in Haughton, S.H., ed.,

Geology of some ore-reposits in Southern Africa, 1.

Geol. Soc. S. Afr.